A subset of group A-like *var* genes encodes the malaria parasite ligands for binding to human brain endothelial cells

Antoine Claessens[a], Yvonne Adams[a,1], Ashfaq Ghumra[a,1], Gabriella Lindergard[a], Caitlin C. Buchan[a], Cheryl Andisi[b], Peter C. Bull[b], Sachel Mok[c], Archna P. Gupta[c], Christian W. Wang[d], Louise Turner[d], Mònica Arman[a], Ahmed Raza[a], Zbynek Bozdech[b], and J. Alexandra Rowe[a,2]

[a]Centre for Immunity, Infection and Evolution, Institute of Immunology and Infection Research, School of Biological Sciences, University of Edinburgh, Edinburgh, EH9 3JT, United Kingdom; [b]Kenya Medical Research Institute-Wellcome Laboratories, 80108 Kilifi, Kenya; [c]School of Biological Sciences, Nanyang Technological University, Republic of Singapore 637551; [d]Centre for Medical Parasitology, Department of International Health, Immunology, and Microbiology, Faculty of Health and Medical Science, University of Copenhagen, and Department of Infectious Diseases, Copenhagen University Hospital (Rigshospitalet), 1014 Copenhagen K, Denmark

Edited by Russell Howard, Oakbio Inc., Sunnyvale, CA, and accepted by the Editorial Board April 25, 2012 (received for review December 13, 2011)

Cerebral malaria is the most deadly manifestation of infection with *Plasmodium falciparum*. The pathology of cerebral malaria is characterized by the accumulation of infected erythrocytes (IEs) in the microvasculature of the brain caused by parasite adhesins on the surface of IEs binding to human receptors on microvascular endothelial cells. The parasite and host molecules involved in this interaction are unknown. We selected three *P. falciparum* strains (HB3, 3D7, and IT/FCR3) for binding to a human brain endothelial cell line (HBEC-5i). The whole transcriptome of isogenic pairs of selected and unselected parasites was analyzed using a variant surface antigen-supplemented microarray chip. After selection, the most highly and consistently up-regulated genes were a subset of group A-like *var* genes (*HB3var3*, *3D7_PFD0020c*, *ITvar7*, and *ITvar19*) that showed 11- to >100-fold increased transcription levels. These *var* genes encode *P. falciparum* erythrocyte membrane protein (PfEMP)1 variants with distinct N-terminal domain types (domain cassette 8 or domain cassette 13). Antibodies to HB3var3 and PFD0020c recognized the surface of live IEs and blocked binding to HBEC-5i, thereby confirming the adhesive function of these variants. The clinical in vivo relevance of the HBEC-selected parasites was supported by significantly higher surface recognition of HBEC-selected parasites compared with unselected parasites by antibodies from young African children suffering cerebral malaria (Mann–Whitney test, $P = 0.029$) but not by antibodies from controls with uncomplicated malaria (Mann–Whitney test, $P = 0.58$). This work describes a binding phenotype for virulence-associated group A *P. falciparum* erythrocyte membrane protein 1 variants and identifies targets for interventions to treat or prevent cerebral malaria.

adherence | pathogenesis | sequestration

Cerebral malaria (CM) is the most serious outcome of a *Plasmodium falciparum* infection, leading to death in 10–20% of cases and to long-term neurological deficits in others (1). The hallmark of the disease is microvascular sequestration, a process in which *P. falciparum*–infected erythrocytes (IEs) cytoadhere to endothelial cells, leading to microvascular obstruction, acidosis, hypoxia, and release of inflammatory cytokines (reviewed in ref. 2). Currently there is no specific treatment for CM other than standard antimalarial drugs and supportive therapies such as fluid replacement (3). The molecular mechanisms underlying CM are not understood, partly because of the lack of an appropriate animal model (4). However, human brain microvascular endothelial cell (HBEC) lines, such as HBEC-5i (5), can be used to study malaria host–parasite interactions, providing an in vitro model for CM (6–9). Despite the existence of this in vitro model, the parasite ligand(s) and host-cell receptor(s) mediating the interaction between IEs and brain endothelial cells remain unknown.

Previous work has identified variant surface antigens (VSA) such as *P. falciparum* erythrocyte membrane protein 1 (PfEMP1) as the parasite ligands mediating adhesion to a variety of receptors on human cells (10, 11). The PfEMP1 family is encoded by 50–60 *var* genes per parasite isolate (12). Although the sequence of each *var* gene is unique, all variants start with an N-terminal segment (NTS) and are followed by a succession of Duffy binding-like (DBL) and cysteine-rich interdomain region (CIDR) domains. These domains can be categorized into subtypes by the presence of short, conserved amino acid motifs, the rest of the sequence being highly polymorphic (13). The *var* gene family is subdivided into three main subgroups, A, B, and C, based on semiconserved upstream sequences (12). All group A *var* genes are located near the telomeres, all group C *var* genes are near the centromeres, and group B *var* genes can be found in either location. The *var* gene groups have functional and clinical significance. Group B and C *var* genes encode PfEMP1 variants that bind CD36 (14, 15) and are linked to nonvirulent clinical disease, whereas group A *var* genes encode non–CD36-binding variants linked to severe clinical disease including CM (16–19). Some group A *var* genes encode PfEMP1 variants that bind to uninfected erythrocytes to form rosettes (20–25); however, the adhesion phenotype of the majority of group A variants is unknown currently.

Although, because of their position on the surface of IEs, PfEMP1 encoded by *var* genes and other VSA such as rifins and stevors are the major candidates for parasite adhesion ligands, it remains possible that other parasite adhesins remain to be discovered. We investigated the whole transcriptome of parasites selected for binding to HBEC-5i cells to identify the parasite ligands for adhesion. We postulated that the parasite ligand(s) necessary for binding to HBEC-5i would be expressed at a higher level in

Author contributions: A.C., Z.B., P.C.B., and J.A.R. designed research; A.C., Y.A., A.G., G.L., C.C.B., C.A., S.M., A.P.G., C.W.W., M.A., and A.R. performed research; G.L., L.T., and Z.B. contributed new reagents/analytic tools; A.C., Y.A., A.G., G.L., C.C.B., C.A., P.C.B., S.M., A.P.G., C.W.W., M.A., and J.A.R. analyzed data; and A.C., Y.A., A.G., G.L., C.A., P.C.B., S.M., A.P.G., C.W.W., L.T., M.A., Z.B., and J.A.R. wrote the paper.

The authors declare no conflict of interest.

This article is a PNAS Direct Submission. R.H. is a guest editor invited by the Editorial Board.

Freely available online through the PNAS open access option.

Data deposition: The microarray data reported in this paper have been deposited in the Gene Expression Omnibus (GEO) database, www.ncbi.nlm.nih.gov/geo (accession no. GSE32211).

[1]Y.A. and A.G. contributed equally to this work.

[2]To whom correspondence should be addressed. E-mail: Alex.Rowe@ed.ac.uk.

This article contains supporting information online at www.pnas.org/lookup/suppl/doi:10.1073/pnas.1120461109/-/DCSupplemental.

selected (adherent) than in unselected (nonadherent) parasites and tested the hypothesis using microarray technology (25).

Results

Selection of *P. falciparum* for Binding to HBEC-5i. Preliminary experiments indicated that in vitro cultures of *P. falciparum* adhere poorly to HBEC-5i (Fig. 1*A*, *Left*). Four *P. falciparum* laboratory strains (HB3, 3D7, IT, and Dd2) were selected for binding to HBEC-5i cells by repeated panning (9). After five to seven rounds of selection, HBEC-5i–adherent lines were obtained from the HB3 (Fig. 1*A*, *Right*), 3D7, and IT strains. The *P. falciparum* strain Dd2 did not increase in adhesion to HBEC-5i cells even after five rounds of selection, suggesting that Dd2 lacks (or is unable to transcribe or transport) the necessary parasite ligand or that the lack of knobs in Dd2 prevents adhesion (26). HB3 was selected twice independently on HBEC-5i to provide a replicate for subsequent experiments (HB3-HBEC1 and 2). HB3 also was selected on TNF-activated HBEC-5i (HB3-HBEC-TNF) to investigate whether different parasite ligands would be selected on cytokine-stimulated and resting endothelial cells.

To assess the relevance of HBEC-5i selection for primary human tissues, HB3-HBEC parasites were tested for adhesion to primary endothelial cells derived from brain, dermal, and lung tissues (ScienCell). In all cases the selected parasites showed enhanced binding to primary endothelial cells (>10-fold greater adhesion of selected than unselected parasites) (Fig. 1*B*). Furthermore, HBEC-5i–binding IEs that were physically detached from HBEC-5i cells and then incubated with other endothelial cell lines showed strong binding (Fig. 1*C*), excluding the possibility that subpopulations of parasites bound to the different cell lines. These data show that the HBEC-5i–selected phenotype is relevant for primary human tissues and indicates that the host receptor is present on endothelia from diverse sources, consistent with sequestration of IEs in multiple endothelial beds in CM patients in vivo (27). Neither unselected nor HB3-HBEC–selected parasite lines bound above background levels to COS-7 cells, showing that the selected parasites do not bind nonspecifically to all cell types.

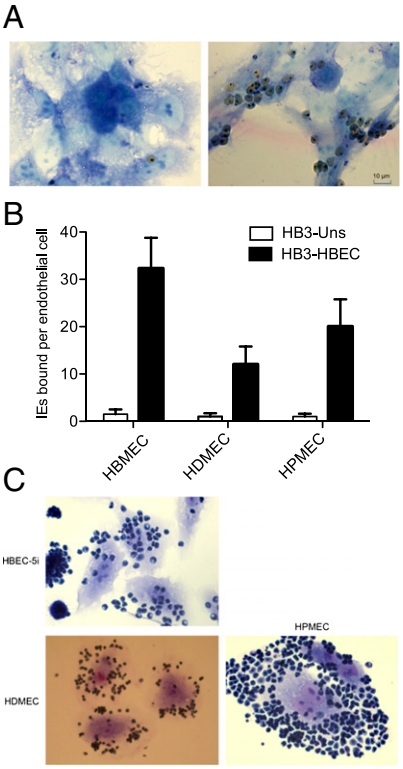

Fig. 1. Selection of *P. falciparum* IEs for adhesion to HBMEC. (*A*) Unselected *P. falciparum* lines (e.g., HB3 shown here) show only minimal binding to HBEC-5i cells (*Left*). After five rounds of panning, adherent parasites are selected (*Right*). The cells were fixed with glutaraldehyde, stained with Giemsa, and visualized by microscopy at 1,000× magnification. (*B*) Binding of selected (HB3-HBEC) and unselected (HB3-Uns) parasite lines to primary endothelial cells from human brain (HBMEC), skin (HDMEC), and lung (HPMEC). Means + SE from triplicate wells are shown. (*C*) Rebinding of HBEC-5i–adherent IEs that were detached mechanically from HBEC-5i cells and then reincubated with HBEC-5i cells (positive control), HDMEC, or HPMEC.

Adhesion Phenotype of HBEC-5i–Selected Parasites. The other adhesion properties of the selected parasites were examined. The selected lines from all three strains did not form rosettes (*SI Appendix*, Fig. S1*A*), and platelet-mediated clumping was reduced significantly after selection for HBEC-5i binding (*SI Appendix*, Fig. S1*B*). HB3-HBEC–selected parasites showed significantly lower binding to CD36 and ICAM-1 than did HB3–unselected parasites (*SI Appendix*, Fig. S1*C*), and there was no increase in binding to any known *P. falciparum* adhesion receptor, including fractalkine, PECAM-1, P-selectin, E-selectin, VCAM-1, integrin αVβ3, thrombospondin, NCAM, fibronectin, heparin, chondroitin sulfate A, hyaluronic acid, gC1qR, or heparan sulfate (*SI Appendix*, Fig. S1*C* and Table S1). IT-HBEC–selected parasites also showed significantly lower binding to CD36 than did IT–unselected parasites, and the only minor but statistically significant increase was in binding to gC1qR (*SI Appendix*, Fig. S1*D*), although absolute levels of binding remained low. gC1qR has been implicated primarily as a platelet-mediated clumping receptor for *P. falciparum*, although it also is expressed on endothelial cells (28). IT-HBEC parasites had a clumping frequency of <2%; therefore it seems unlikely that gC1qR is a major receptor for these parasites. Adhesion-blocking antibodies to CD36 (29) and ICAM-1 (30) had no effect on binding of HBEC-selected parasites to HBEC-5i (*SI Appendix*, Fig. S1*E*), thus further excluding a role for these receptors in HBEC-5i binding. Therefore we were unable to identify the HBEC-5i receptor(s) used by the HBEC-selected parasite lines, and HBEC-5i binding may involve an unknown host endothelial receptor.

We also examined knob positivity in the selected and unselected parasite lines, because lack of knobs is known to influence parasite adhesion properties (26). We found that the percentage of knob-positive IEs in the selected and unselected lines of each strain did not differ significantly (mean percent of knob-positive IE (SE) for HB3-HBEC–selected, 62.5 (2.3) and –unselected, 65.0 (1.7), $P = 0.41$; IT-HBEC–selected, 69.3 (2.5) and –unselected, 68.3 (2.7), $P = 0.79$; 3D7-HBEC–selected, 54.0 (1.5) and –unselected, 55.5 (1.7), $P = 0.53$; unpaired t test in each case). Therefore, the presence or absence of knobs is unlikely to explain the differences in HBEC-5i adhesion between the selected and unselected parasite strains.

Whole-Transcriptome Analysis Identifies a Subset of Group A *var* Genes as Being Highly Transcribed in HBEC-5i–Selected Parasites. We used a VSA-supplemented microarray chip to examine the whole transcriptome of selected and unselected parasites, with the aim of identifying candidate parasite adhesion ligands as gene(s) whose transcriptional levels increased markedly after selection (25). The VSA-supplemented chip contains oligonucleotide probes for all the VSA genes (*var, rif*, and *stevor*) from the HB3, IT, and Dd2 strains (25) added to the existing 3D7-based chip (31). Isogenic pairs of selected and unselected *P. falciparum* parasite cultures were synchronized (*SI Appendix*, Table S2), and RNA samples were collected every 8 h for 48 h. The selected and unselected parasites were at similar levels of maturity during the time-course experiment, as shown by Giemsa smear (*SI Appendix*, Fig. S2) and by strongly positive Pearson correlation coefficients when data from all oligonucleotide

probes at each time point for selected and unselected parasites were compared (*SI Appendix*, Fig. S3; see exceptions for time point 3 of HB3-HBEC-TNF and time point 6 of IT-HBEC, whose data should be interpreted with caution).

The level of transcription of each gene in selected parasites was compared with that in unselected parasites and was expressed as a fold expression ratio. In HB3, the gene with the most markedly and consistently increased transcription in selected parasites was a group A *var* gene, *HB3var3* (Fig. 2 *A–D* and *G*). There were five oligonucleotide probes on the microarray chip for this gene, and all five showed strongly increased hybridization signals in HB3-HBEC1 and HB3-HBEC2 compared with unselected HB3 (Fig. 2 *B* and *C*). Taking an average of all five probes, *HB3var3* was up-regulated in selected parasites by up to 61-fold (Fig. 2*G*). (By "up-regulated" we mean that the amount of mRNA for a particular gene was increased in selected compared with unselected parasites.) Selection of HB3 parasites on TNF-activated HBEC-5i also resulted in a parasite population with increased transcription of *HB3var3* (Fig. 2 *D* and *G*). Multiple other *var* genes were up-regulated at time point 3 in the parasites selected on TNF-activated HBEC-5i, but the upregulation of these genes may have been caused by poor synchronization between selected and unselected parasites at this time point (*SI Appendix*, Fig. S3).

In 3D7, a single group A *var* gene, *PFD0020c*, showed the most marked and consistent increase in transcription after selection (Fig. 2 *E* and *G*). All six oligonucleotide probes to *PFD0020c* showed a similar pattern. In the IT strain, two *var* genes, *ITvar7* (group A) and *ITvar19* (group B), showed highly increased transcription after selection (Fig. 2*F*). The five probes specific to each of these two genes showed, on average, an up-regulation of 10- to more than 100-fold (Fig. 2*G*).

When the five selections are considered together, the microarray data for the *var* gene family are striking. In all five selections, one or two *var* genes show markedly increased transcription in the selected parasites, but multiple other *var* genes are down-regulated. At time point 3 (16–24 h postinvasion), there is an 11- to 320-fold increase in *HB3var3*, *PFD0020C*, *ITvar9*, and *ITvar19* in the selected populations (Fig. 2*G*). No other *var* gene was up-regulated by more than twofold across more than one time point.

Quantitative real-time PCR (qPCR) with specific primers to the *var* genes of each parasite strain confirmed the up-regulation detected by microarray (Fig. 2*G*) and did not detect any other up-regulated *var* genes. Expression profiling by RT-PCR with universal primers to the *var* gene DBLα region (32, 33) also identified the same set of up-regulated *var* genes (*SI Appendix*, Fig. S4 *A–D*), confirming that all three methods are comparable. RT-PCR experiments on HB3 parasites selected for binding to human dermal microvascular endothelial cells (HDMEC) and human pulmonary microvascular endothelial cells (HPMEC) showed that the group A *var* gene up-regulated with HBEC-5i (*HB3var3*) also was up-regulated following selection on other endothelial types (*SI Appendix*, Fig. S4*E*).

***Rif* Genes Located Head-to-Head with the *var* Gene Ligand Candidates Are Up-Regulated.** In the *rif* family, three genes showed increased transcription by threefold or more in at least one time point in all three HB3 selections (Fig. 3*A*). Only one of these genes, *HB3RifA_081*, showed a substantial, eight- to 100-fold increase (Fig. 3*B*). Interestingly, this *rif* gene is located next to *HB3var3*, on the opposite strand, and is transcribed in the opposite direction. Thus, the selection of HB3 parasites on HBEC-5i, with or without prior activation with TNF, led to the increased transcription of *HB3var3* and its "head-to-head" *HB3_RifA_081* gene. No *stevor* gene was up-regulated by threefold or more in all three HB3-derived selections.

In 3D7-HBEC, the most highly up-regulated *rif* gene was *PFD0025w* (Fig. 3*B* and *SI Appendix*, Fig. S5*A*). Again, this *rif* gene is located head-to-head with the most highly transcribed *var* gene, *PFD0020c.* Several other *rif* genes and four *stevor* genes showed more than threefold up-regulation in at least one time point (*SI Appendix*, Fig. S5*A*). These data are each based on a single probe (because of the small size of *rif* and *stevor* genes) and a single experiment; therefore further replicates would be required to determine whether these increases are consistent. In IT-HBEC, five *rif* genes and one *stevor* gene showed more than threefold up-regulation in a single time point (*SI Appendix*, Fig S5*B*). No expression data were available for *IT4rifA_044*, the *rif* gene found head to head with *ITvar7*. This lack of data may mean that this gene is not transcribed above background levels in one of the parasite populations or could be the result of a technical problem, such as misprinting of the oligonucleotide probe. The other up-regulated *var* gene in IT parasites, *ITvar19,* does not have a head-to-head *rif* gene, because these head-to-head arrangements are found only with group A *var* genes.

To confirm the up-regulation of the specific head-to-head *rif* genes in the HB3 and 3D7 strains, and to examine further the transcription of *IT4rifA_044*, the *rif* gene found head-to-head with *ITvar7*, we carried out real-time qPCR with *rif*-specific primers (34). This evaluation confirmed the up-regulation of *HB3_RifA_081* in HB3-selected parasites and *PFD0025w* in 3D7-selected parasites (Fig. 3*B*). Furthermore, the data showed a 446-fold increase in *IT4rifA_044* in IT-selected parasites (Fig. 3*B*).

Taken together, these data indicate that selection for binding to HBEC-5i leads to increased transcription of specific group A *var* genes and that the *rif* genes located head-to-head with these *var* genes are up-regulated also. Therefore, the genes *HB3rifA_081*, *PFD0025w*, and *IT4rifA_044* also should be considered as encoding potential parasite ligands for HBEC-5i binding, given the known location of rifins on the surface of IEs (35).

Some Exported Proteins Show Increased Transcription in HBEC-Selected Parasites. The four *var* genes identified above and their accompanying *rif* genes are by far the most highly and consistently up-regulated genes after selection. However, other non-VSA genes could be involved in cytoadherence to HBEC-5i. The vast majority of non-VSA genes have a sequence that is virtually identical from one strain to another; therefore the three strains (HB3, 3D7, and IT) can be considered as replicates of each other (36). Using the arbitrary cutoff of a twofold increase in at least one time point, 15 non-VSA genes were found to be up-regulated, and 58 non-VSA genes were down-regulated in all five selections (*SI Appendix*, Figs. S6 and S7). No specific functional pathways were statistically significantly up-regulated by functional enrichment analysis. Furthermore, no non-VSA genes showed increases in transcription comparable in intensity or consistency to the up-regulated *var* genes (*SI Appendix*, Fig. S6 and Fig. 2). Only one gene was up-regulated by at least threefold in all five selections: *PF14_0472*, a member of the Plasmodium helical interspersed subtelomeric (PHISTa) family (37). Six other up-regulated genes encode proteins predicted or proven to be exported: *P. falciparum* erythrocyte membrane protein 3 (*PfEMP3*) (38), ring-IE surface antigen (*RESA-1*) (39), membrane associated histine-rich protein 1 (*MAHRP-1*) (40), and three others with a Pexel motif: *PF14_0740*, *PF11_0035*, and *PFF0055w* (37). These six genes and *PF14_0472* are up-regulated at time point 3 (16–24 h postinvasion) in almost all selections, indicating that they could be translated in time for cytoadherence at the pigmented trophozoite stage.

Of the 58 down-regulated genes, 11 were down-regulated by at least threefold in at least one time point (*SI Appendix*, Fig. S7). Intriguingly, 41 of the 58 down-regulated genes encode proteins proven or predicted to be involved with merozoite invasion. Indeed, a functional enrichment analysis revealed the merozoite invasion pathway to be highly enriched ($P \sim 0$) (*SI Appendix*, Table S3). In other words, the selection of parasites for binding to HBEC-5i resulted in a statistically highly significant decrease

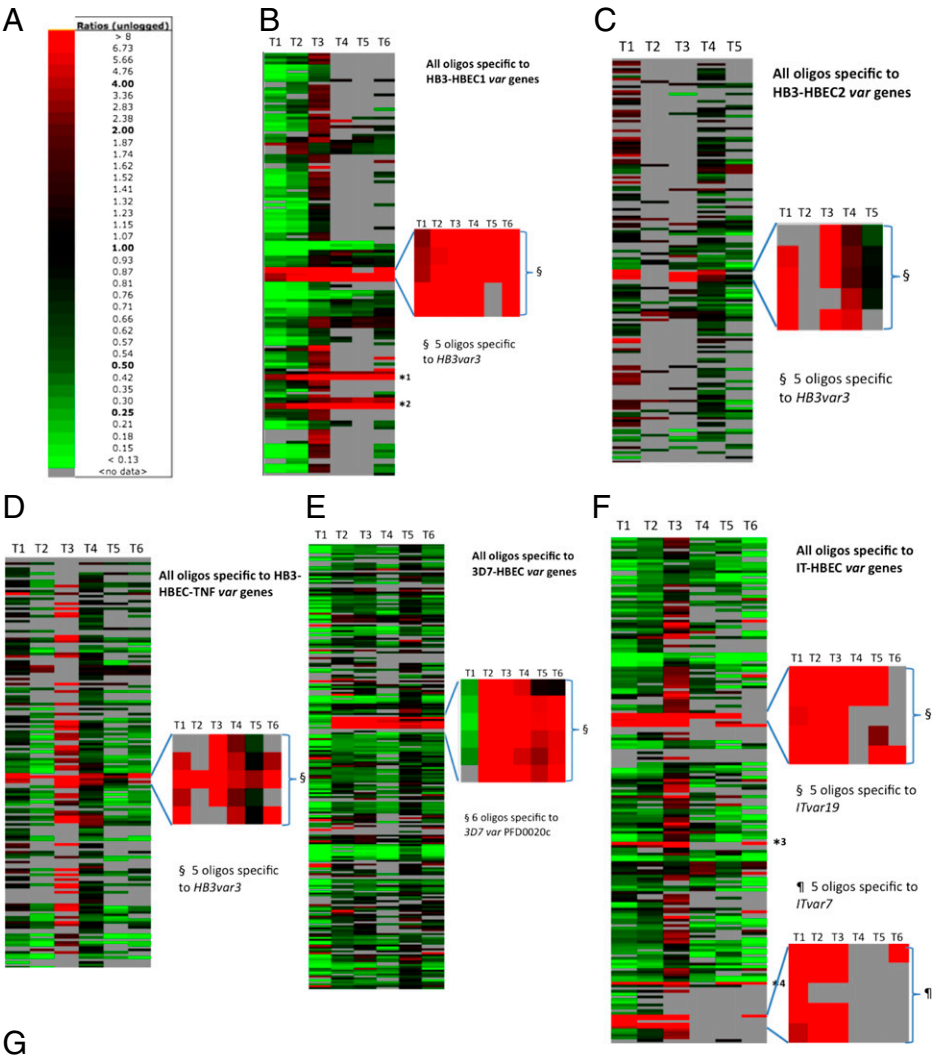

G

	T1	T2	T3	T4	T5	T6		qRT-PCR
HBEC1: *HB3var3*	8.5	13.4	34.1	61.0	9.8	25.1		ND
HBEC2: *HB3var3*	6.4	NA	11.2	3.0	0.8	NA		ND
HB3-HBEC-TNF: *HB3var3*	5.1	2.3	37.5	3.5	1.3	5.6		24.5
3D7-HBEC: *PFD0020c*	0.4	22.0	19.6	7.0	4.2	6.3		17.7
IT-HBEC: *IT4var7*	13.1	14.2	177.2	NA	NA	10.3		454.3
IT-HBEC: *IT4var19*	9.2	32.8	319.2	14.7	12.7	13.8		143.8

Fig. 2. Microarray analysis indicates that a subset of group A *var* genes shows markedly increased transcription after selection for HBEC-5i binding. (*A*) Color scale showing the fold expression ratios of gene transcription in selected versus unselected parasites. (*B–F*) *Var* gene transcription throughout the 48 h asexual life cycle in HBEC-5i–selected and unselected *P. falciparum* strains HB3: (*B*) replicate 1, HB3-HBEC1; (*C*) replicate 2, HB3-HBEC2; (*D*) HB3 on TNF-stimulated cells;,HB3-HBEC-TNF; (*E*) 3D7-HBEC; and (*F*) IT-HBEC. Each row represents a different oligonucleotide probe, and each column is a time point. T1 = maximum parasite maturity, 8 h postinvasion; T2 = 16 h; T3 = 24 h; T4 = 32 h; T5 = 40 h; T6 = 48 h. Red rectangles indicate higher transcription in the selected than in the unselected population. Green rectangles indicate higher transcription in the unselected population. A gray rectangle indicates no *var* gene transcription detected above background level in at least one parasite population. For each selection, the most highly up-regulated *var* gene(s) has been zoomed out. All oligonucleotide probes are shown except for those with no transcription above background level at any time point. A few *var* genes have sections of sequence identical to other *var* genes within the same strain (62). For example, the second half of *HB3var3* shows similarities with *HB3var5* and *HB3var46p*. Therefore, some oligos are not unique to a single sequence. *1, oligos HB3var46p_2 and HB3var46p_3 match the *HB3var3* gene. Oligos HB3var46p_0 and HB3var46p_1 are unique to *HB3var46p* and are not up-regulated. *2, oligos HB3var5_2 and HB3var5_3 match *HB3var3*. Oligos HB3var5_0 and HB3var5_1 are unique to *HB3var5* and are not up-regulated. *3, oligos ITvar32_2, ITvar32_3, and *4, oligo ITvar6_0 - match *ITvar19*. However, other oligos specific to *ITvar32* (ITvar32_0 and 1) and *ITvar6* (ITvar6_1, 2 and 3) are not up-regulated. (*G*) Expression fold ratios (unlogged) of the most up-regulated *var* genes in each selection. Numbers represent the average of all oligonucleotide probes specific to that gene. The last column indicates real-time qPCR data obtained from RNA at late ring stage. NA, not available (i.e., no transcription above background level was detected in at least one parasite population); ND, not determined.

in transcription of invasion-related genes. This decrease in transcription occurred during time points 1–5 but not at time point 6 (schizogony) when invasion genes primarily are expected to be transcribed and translated. Thus, the actual amounts of invasion proteins necessary for merozoites to invade red blood cells may remain the same in HBEC-5i–selected parasites.

A

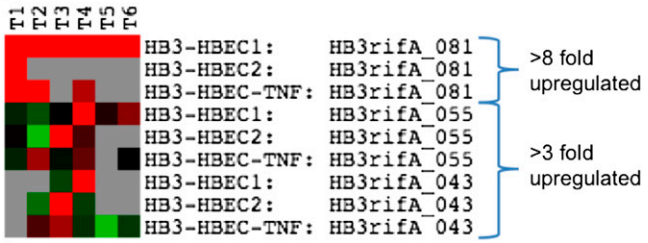

B

	T1	T2	T3	T4	T5	T6	qRT-PCR
HB3-HBEC1: *HB3rifA_081*	15.4	18.9	17.9	99.9	16.0	32.9	ND
HB3-HBEC2: *HB3rifA_081*	10.1	NA	NA	NA	NA	NA	ND
HB3-HBEC-TNF: *HB3rifA_081*	7.8	16.0	NA	3.8	NA	NA	11.1
3D7-HBEC: *rif_PFD0025w*	0.8	NA	15.6	NA	0.9	1.3	22.6
IT-HBEC: *IT4rifA_044*	NA	NA	NA	NA	NA	NA	446

Fig. 3. The *rif* genes located head-to-head with the up-regulated *var* genes are up-regulated also. (*A*) HB3 *rif* genes up-regulated by at least threefold in all HB3-derived strains. Because of the small size of *rif* genes (1–2 kbp), there was only one oligonucleotide probe per gene on the microarray chip. Color scale is as in Fig. 2. (*B*) Expression fold ratios of the *rif* genes located head-to-head with the most up-regulated *var* genes in each selection. The last column indicates real-time qPCR data, obtained from RNA at late ring stage. NA, not available (i.e., no transcription above background level was detected in at least one parasite population); ND, not determined.

Taken together, examination of the entire transcriptome of three *P. falciparum* strains selected for adhesion to HBEC-5i identifies a subset of group A *var* genes and their head-to-head *rif* genes as the most likely candidates for adhesion ligands because of their markedly increased transcription after selection.

Up-Regulated *Var* Genes Show Similarities in PfEMP1 Architecture. Examination of the *var* genes up-regulated in HBEC-5i–selected parasites reveals that they encode PfEMP1 variants that are diverse in sequence (32–46% amino acid identity between each pair) (*SI Appendix*, Table S4). However, the up-regulated variants do show similarities in PfEMP1 architecture (Fig. 4). As expected for group A *var* genes, *HB3var3*, *PFD0020c*, and *ITvar7*, all encode variants with a DBLα1 domain at the N-terminus, whereas the group B *ITvar19* variant has a DBLα2 domain (Fig. 4). Despite its group B upstream region, the *ITvar19*-encoded variant has some group A-like features: It is large (with seven extracellular domains, compared with four for a typical group B variant) and has a CIDRα1 domain (usually found in group A variants). The presence of the CIDRα1 domain, which is uncommon (present in <10% of all *var* genes) is the most obvious distinguishing feature of the four adhesion ligand candidates. DBLα1 and CIDRα1 domains recently have been classified into subgroups on the basis of sequence homology (41). Both HB3var3 and ITvar7 have the N-terminal domain pair DBLα1.7/CIDR1α1.4, also known as "domain cassette (DC) 13." [Domain cassettes are sets of PfEMP1 domains that usually occur together (41).] Of seven *P. falciparum* strains whose *var* gene repertoires have been fully sequenced and classified, most strains have only one variant with DC13, and these variants are all group A *var* genes that show PfEMP1 architecture similar to that of HB3var3 and ITvar7 (41). Thus, DC13-type variants, including HB3var3 and ITvar7, may represent functionally similar alleles in different parasite strains. PFD0020c and ITvar19 have different DBLα types, but they share very similar CIDRα1.1 domains with 74% amino acid identity (but only 39–43% identity with CIDRα1.4 of HB3var3 and ITvar7) (*SI Appendix*, Table S4). Other sequenced strains usually have only one variant with a CIDRα1.1 domain, and most of these strains are group B PfEMP1 variants with PfEMP1 architecture similar to that in ITvar19, represented by DC8 (41). PFD0020c has three of the four domains usually found in DC8, differing only in the first DBL domain (Fig. 4).

The HB3var3 variant is identical to HB3var5 from the DBLγ domain to the end of the extracellular region. The fact that HB3var3 but not HB3var5 was up-regulated after selection for binding to HBEC-5i suggests that the functional binding region includes the first three domains (NTS-DBLα-CIDRα-DBLβ) that differ in HB3var3 and HB3var5.

Antibodies Against HB3var3 Inhibit Adhesion of HB3-HBEC to HBEC-5i. The transcriptional patterns shown above combined with the known adhesion properties of PfEMP1 make the PfEMP1 variants encoded by *HB3var3*, *PFD0020c*, *ITvar7*, and *ITvar19* the most likely candidate parasite adhesion ligands for HBEC-5i binding. To test the hypothesis that this subset of group A-like *var* genes encodes the parasite ligands for adhesion to HBEC-5i, we raised antibodies to specific PfEMP1 domains.

The NTS-DBLα1 and the NTS-DBLα1-CIDRα1 (hereafter called the "di-domain") from HB3var3 were expressed as recombinant proteins in *Escherichia coli.* For NTS-DBLα1, the recombinant protein was mostly of the expected molecular weight (54.1 kDa) and showed a shift upon reduction, indicating the presence of disulfide bonds in the recombinant protein (Fig. 5*A*, *Left*). For the di-domain, much of the protein was degraded, although some protein at the expected molecular weight (88.2

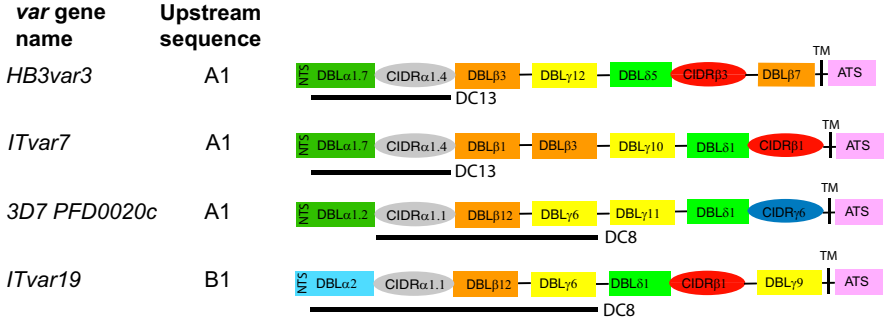

Fig. 4. PfEMP1 architecture of variants up-regulated after HBEC-5i selection. ATS, acidic terminal segment; CIDR, cysteine-rich interdomain region; DBL, Duffy binding-like domain; DC13, domain cassette 13; DC8, domain cassette 8; NTS, N-terminal segment. Pairwise amino acid identities between domains are shown in *SI Appendix*, Tables S4 and S5.

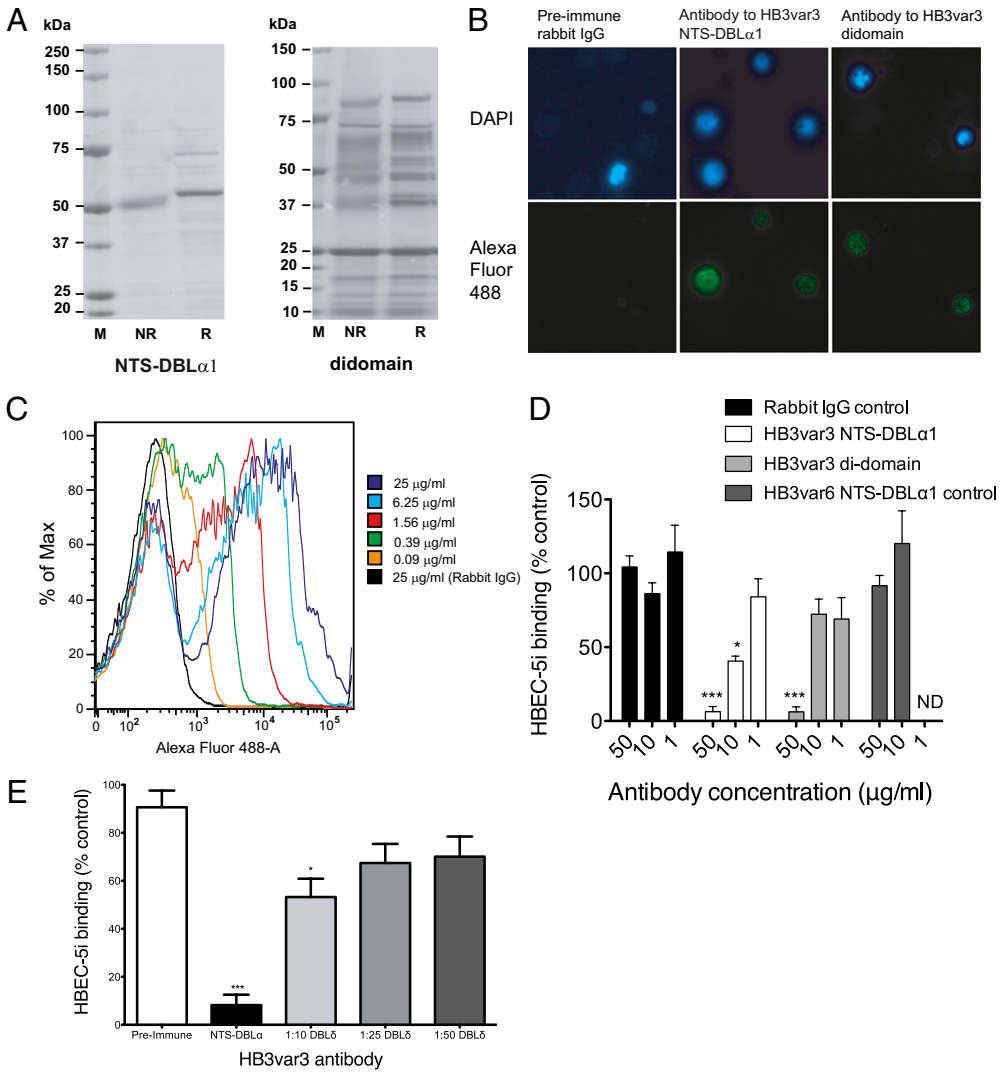

Fig. 5. Antibodies against HB3var3 inhibit adhesion of HB3-HBEC to HBEC-5i cells. (*A*) SDS/PAGE showing recombinant NTS-DBLα1 and di-domain (NTS-DBLα1-CIDRα1) domains from HB3var3 expressed in *E. coli*. (*B*) Immunofluorescence assay with antisera to HB3var3 (1/100 dilution) showing punctate surface fluorescence on live IEs. IEs are shown by DAPI staining of the parasite nuclei. PfEMP1 antibody was detected with highly cross-absorbed goat anti-rabbit IgG Alexa Fluor 488 (1/1,000). (*C*) Titration of anti-HB3var3 antibodies (purified total IgG) against live HB3-HBEC IEs by flow cytometry. (*D*) Inhibition of HB3-HBEC binding to HBEC-5i cells by antibodies to HB3var3 NTS-DBLα1 and di-domain. Means and SD from quadruplicate wells of a representative experiment are shown. Binding is compared with control wells with no added IgG. Negative controls are nonimmunized rabbit IgG and IgG raised to the NTS-DBLα1 domain of a rosette-mediating group A PfEMP1 variant (HB3var6). A significant decrease in adhesion was seen in the presence of HB3var3 antibodies ($P < 0.0001$, ANOVA). ***$P < 0.001$, *$P < 0.05$, Tukey's multiple comparison test. (*E*) Inhibition of HB3-HBEC binding to HBEC-5i cells by antibodies to HB3var3 DBLδ5. Mean and SE from three independent experiments are shown. Binding is compared with control wells with no added IgG. The negative control is preimmune serum from the rabbit used to raise DBLδ5 antibodies. A significant decrease in adhesion was seen in the presence of HB3var3 antibodies ($P < 0.0001$, ANOVA). *$P < 0.05$, ***$P < 0.001$, Tukey's multiple comparison test.

kDa), and which showed a shift upon reduction, was obtained (Fig. 5*A*, *Right*).

Antisera to HB3var3 NTS-DBLα1 and the di-domain showed punctate surface fluorescence of live HB3-HBEC IEs by immunofluorescence assay (IFA) (Fig. 5*B*) typical of PfEMP1 antibodies (23). Rabbit preimmune sera and nonimmunized rabbit control sera were negative by IFA. Total IgG were purified from the antiserum and used at fourfold dilutions in flow cytometry to determine the end titer (here defined as the lowest concentration of total IgG to stain in >50% of live IEs). The HB3var3 NTS-DBLα1 antibodies gave surface reactivity down to 0.39 μg/mL of total IgG (Fig. 5*C*), and the di-domain antibodies gave surface reactivity down to 1.56 μg/mL of total IgG. The HB3var3 NTS-DBLα1 antibodies were tested at 400 μg/mL for live IE surface reactivity with other *P. falciparum* strains selected for a range of different adhesion phenotypes (24). The antibodies did not show surface reactivity with HB3-unselected parasites, 3D7-HBEC, 3D7-unselected, IT-HBEC, IT-unselected, six *P. falciparum* rosetting strains, or 12 clinical isolates (data are shown in figures 4b and 6a of ref. 24, in which the non-Ros group A control is HB3var3 NTS-DBLα1 antibody). Therefore, the HB3var3 NTS-DBLα1 antibodies are highly variant- and strain-specific and show surface reactivity only with the homologous parasite line HB3-HBEC expressing the HB3var3 PfEMP1 variant.

To determine whether the HB3var3 PfEMP1 variant is the parasite ligand for binding to HBEC-5i, the effect of HB3var3 antibodies on adhesion was examined. Both NTS-DBLα1 and di-domain antibodies inhibited binding to HBEC-5i compared with control nonimmunized rabbit IgG (Fig. 5*D*). Polyclonal rabbit IgG raised against a PfEMP1 variant not involved in HBEC-binding

(against the NTS-DBLα1 domain of the rosette-mediating HB3var6 group A PfEMP1 variant) (24) showed no inhibition of binding (Fig. 5*D*). We also tested antiserum raised against another recombinant domain of the HB3var3 variant (DBLδ5) produced in baculovirus (42). Previous work has shown that antibodies to multiple PfEMP1 domains are able to block adhesion in the case of rosetting parasites (23). The HB3var3 DBLδ5 antiserum showed punctate surface fluorescence with live IEs of HB3-HBEC parasites at 1/25 and 1/100 dilution, whereas the preimmune serum was negative at the same concentrations. The antiserum was negative by IFA against HB3-unselected, 3D7-HBEC, 3D7-unselected, IT-HBEC, and IT-unselected parasites. The antiserum to HB3var3 DBLδ5 showed specific inhibition of adhesion of HB3-HBEC IEs to HBEC-5i, although it was not as effective as NTS-DBLα1 antibody (Fig. 5*E*). Therefore, three different antibody preparations against two distinct domains of the HB3var3 PfEMP1 variant inhibited binding of HB3-HBEC to HBEC5i, confirming that HB3var3 is a parasite adhesion ligand and making it extremely unlikely that antibody cross-reactivity with other molecules on the surface of IEs is responsible for the data shown. None of the antibodies caused agglutination of IEs at the concentrations used in the adhesion inhibition assays.

Antibodies to two distinct domains of the PfEMP1 variant up-regulated in 3D7 parasites, PFD0020c, also were tested for adhesion inhibition. Antibodies to the NTS-DBLα1 domain of PFD0020c (produced in *E. coli*) gave punctate surface fluorescence of 3D7-HBEC live IEs down to 6.25 μg/mL of total IgG, whereas antibodies to DBLγ6 (produced in *Baculovirus*) gave surface reactivity down to 100 μg/mL Both antibodies were variant- and strain-specific and did not show surface reactivity with the IT- or HB3-HBEC–selected or –unselected parasite lines when tested at 400 μg/mL The NTS-DBLα1 antibodies inhibited binding of 3D7-HBEC to HBEC-5i by 52% compared with rabbit IgG control at 50 μg/mL of total IgG, whereas the DBLγ6 antibodies inhibited binding by 64% compared with rabbit IgG control at 250 μg/mL of total IgG ($P < 0.001$, paired *t* test). Therefore, for PFD0020c, two independent antibody preparations to separate domains show variant- and strain-specific surface reactivity and inhibit adhesion of 3D7-HBEC to HBEC-5i, providing evidence that the PFD0020c PfEMP1 variant is the parasite adhesion ligand.

In Vivo Significance of the HBEC-5i–Binding Subset of Group A PfEMP1 Variants. No animal model adequately reflects the pathology and clinical features of severe *P. falciparum* malaria in humans; therefore, it is not possible to test directly whether HBEC-5i–selected parasites cause CM. As an alternative approach to examine the in vivo significance of the HBEC-5i–binding variants, we investigated whether African children suffering from CM develop antibodies that recognize the HBEC-selected parasite lines. Plasma samples from acutely ill or convalescent Kenyan children with CM or uncomplicated malaria (UM) were used to assess surface recognition of live IEs from selected and unselected parasites by flow cytometry. Acute plasma samples collected from both clinical groups at the time of hospital admission (predominantly reflecting prior exposure) showed no significant difference in their reactivity with selected or unselected parasite lines (Fig. 6 *A* and *B*). However, plasma samples from convalescent patients with CM (reflecting antibody responses to the variant causing the clinical episode) showed significantly greater recognition of the HBEC-selected lines than of the unselected lines (Fig. 6*C*). In contrast, plasma samples from convalescent patients with UM did not show differential reactivity with HBEC-selected lines compared with -unselected lines (Fig. 6*D*), although surface reactivity against both HBEC-selected and -unselected lines increased compared with the samples from acutely ill patients (Fig. 6 *B* and *D*). When each parasite strain was considered individually, all three strains showed a trend toward increased recognition of HBEC-selected compared with -unselected parasites in sera from convalescent patients with CM, but the increase was statistically significant only in the 3D7 strain (*SI Appendix*, Fig. S8).

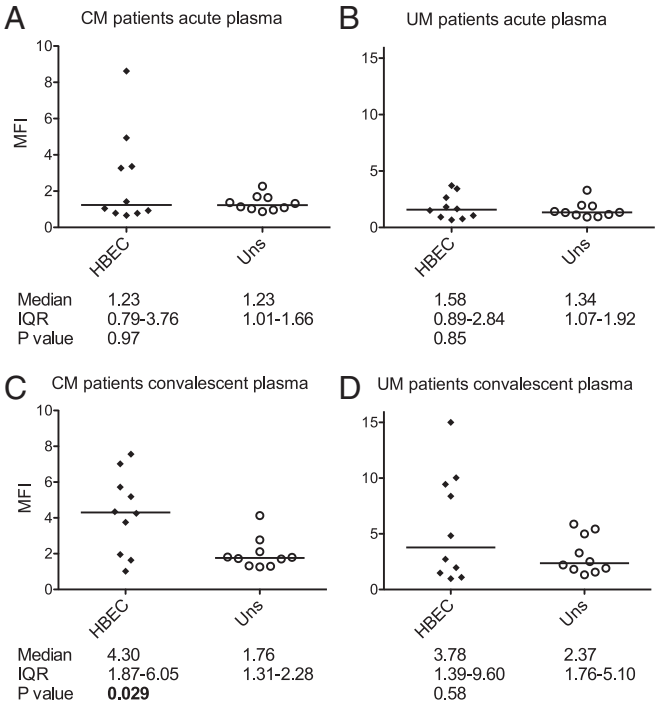

Fig. 6. Recognition of HBEC-selected and -unselected parasites lines by antibodies from African malaria patients. Acute and convalescent plasma samples were collected from 10 patients with CM and 10 age- and date of admission-matched patients with UM. Surface recognition of HBEC-selected and -unselected (uns) parasite lines was tested by flow cytometry. The mean fluorescence intensity (MFI) of the uninfected erythrocyte population was subtracted from the MFI of the IE population to give the specific MFI of the IE population shown on the *y* axis. Each data point represents plasma from one patient. The median of the values from the three individual strains was used to represent the specific recognition of HBEC-selected or -unselected parasites by each plasma sample (the individual strains are shown in *SI Appendix*, Fig. S8). (*A*) Acute plasma from patients with CM. (*B*) Acute plasma from patients with UM. (*C*) Convalescent plasma from patients with CM. (*D*) Convalescent plasma from patients with UM. IQR, interquartile range.

Discussion

In this work we found that a distinct subset of group A-like *var* genes was highly transcribed in three *P. falciparum* strains selected for adhesion to an HBEC line (Fig. 2). The up-regulated genes encode PfEMP1 variants with similar domain structures exemplified by the presence of DC8 (*3D7_PFD0020c* and *ITvar19*) or DC13 (*HB3var3* and *ITvar7*) (Fig. 4). In their companion articles, Avril et al. (43) provide independent confirmation of the up-regulation of DC8 genes following selection on brain endothelial cells, and Lavstsen et al. (44) show DC8 and DC13 genes to be highly differentially transcribed in patients with severe malaria compared with UM controls, confirming the clinical importance of DC8- and DC13-expressing parasites. DC8 genes were differentially transcribed in all clinical forms of severe malaria (CM, severe malarial anemia, and respiratory distress), consistent with our findings and those of Avril et al. (43) that parasites selected for binding to HBEC-5i also could adhere to other primary endothelial cell types, giving the potential to sequester at multiple sites throughout the body in addition to the brain. Taken together, these three studies identify parasites expressing DC8 and DC13 as having high potential for cytoadherence to endothelial cells in the brain and elsewhere and

suggest that DC8 and DC13 PfEMP1 variants may be important targets for interventions to treat or prevent severe malaria.

To confirm the role of DC8 and DC13 PfEMP1 variants in binding to HBEC-5i, we raised antibodies to domains of *HB3var3* and *3D7_PFD0020*. In each case antibodies to two distinct domains showed variant- and strain-specific reactivity with the surface of live IEs and blocked binding of IEs to HBEC-5i (Fig. 5). These data strongly support the identification of the HB3var3 and PFD0020c PfEMP1 variants as parasite adhesion ligands for HBEC-5i binding.

Our examination of the whole transcriptome of three parasite strains showed that the only other highly up-regulated genes after selection for HBEC-5i binding were the *rif* genes located head-to-head with the up-regulated group A *var* genes (Fig. 3). Given the known location of rifins on the surface of IEs (35), it is possible that the rifins could contribute to host cell binding; further experiments will be required to test this possibility. An alternative hypothesis is that the *rif* genes are up-regulated because their transcriptional pattern is linked to the adjacent head-to-head *var* gene. The coregulation of group A *var* genes and their adjacent *rif* genes has been reported previously (34, 45) and also was seen in our proof-of-concept experiment for the VSA-supplemented microarray with rosetting parasites (25).

The microarray approach has the potential to reveal non-VSA genes that could be involved directly or indirectly in cytoadherence, for example by contributing to the trafficking of PfEMP1 to the IE surface. We found only 15 non-VSA genes that were up-regulated by twofold or more in all selections; among these genes were several encoding proteins predicted to be exported into the infected red blood cell cytoplasm (*SI Appendix*, Fig. S6). Two of these genes, *MAHRP-1* and *PF14_0752* (PHISTa), also were modestly up-regulated in IT parasites selected for rosetting (25). An indirect role for MAHRP-1 in cytoadherence already had been demonstrated, because deletion of the gene leads to depletion of surface-exposed PfEMP1 (46). *PF14_0752* is part of the PHISTa subfamily, whose members are specific to *P. falciparum* (37). *PF14_0752* was one of the most highly up-regulated genes in CD36-selected parasites (47), in field isolates (48), and in 3D7 gametocytes (49). Recently a PHISTc family member was shown to bind to the intracellular domain of PfEMP1 (50); however the function of other PHIST family members is unknown and awaits further research.

One of the attractions of the microarray approach is its potential to reveal previously unrecognized parasite adhesion proteins. At first sight, to conclude that the major adhesion ligands are PfEMP1 variants, with a possible contribution from rifins, could be considered disappointing. Similarly, our previous microarray study of rosetting parasites confirmed the marked transcriptional up-regulation of the known parasite rosetting ligand, the PfEMP1 variant encoded by *ITvar9* (20), and did not identify any strong alternative candidates (25). However, we suggest that these data, rather than being disappointing, are important precisely because they provide a convincing demonstration of the importance of PfEMP1 in parasite adhesion that is based on global transcriptional data rather than relying solely on the examination of individual genes and gene families that has characterized previous work.

The demonstration here of up-regulation of a subset of group A-like *var* genes in HBEC-5i–selected parasites fits well with a body of previous work on *var* gene transcription in *P. falciparum* clinical isolates as well as the companion article by Lavstsen et al. (44). The majority of studies addressing the relationship between *var* genes and clinical disease have found an association between group A *var* gene transcription and severe malaria or CM (16–19, 51). Previously, the only known binding phenotype for group A PfEMP1 variants was rosetting (20–23), with two group A domain cassettes (DC11 and DC16) being linked to rosette formation (24). DC16 was not associated with severe malaria in the study by Lavstsen et al. (44) and DC11 was not tested. DC11 is linked to IgM-positive rosetting (24), which probably is the most clinically important rosetting phenotype (52). Further research will be required to study the association between DC11 variants and severe malaria.

ICAM-1 often is cited as an endothelial receptor involved in CM (53); however, its precise role remains uncertain, because several studies show no significant increase in ICAM-1 binding in parasite isolates from patients with CM as compared with controls (54–56). Furthermore, a human ICAM-1 polymorphism that occurs at high frequency in Africa (57) and reduces the ability of *P. falciparum* to bind to ICAM-1 (53, 58) does not protect against CM or severe malaria (59). In the work shown here, although ICAM-1 is expressed on the surface of HBEC-5i, it is not the receptor used by the HBEC-selected parasites because (*i*) in spot-binding assays HBEC-selected parasites did not show increased binding to recombinant ICAM-1 compared with -unselected parasites (*SI Appendix*, Fig. S1 *C* and *D*); (*ii*) ICAM-1 antibodies did not block adhesion of selected parasites to HBEC-5i (*SI Appendix*, Fig S1*E*); and (*iii*) IT-HBEC parasites express *ITvar7* and *ITvar19*, which have been shown to be ICAM-1 nonbinders (60). The endothelial receptor(s) used by the HBEC-5i–selected parasites are currently unknown.

In conclusion, we show that the *P. falciparum* ligands for adhesion to HBEC-5i are a subset of group A-like PfEMP1 variants (DC8 and DC13 type). The clinical relevance of these variants was shown by recognition of HBEC-selected lines by sera from children recovering from CM, thus validating the interaction with HBEC-5i as an in vitro model for CM sequestration. The DC8 and DC13 PfEMP1 variants represent potential targets for interventions to prevent or treat CM.

Materials and Methods

Please see *SI Appendix, Text* for the materials and methods related to the adhesion properties of selected and unselected parasite lines; microarray hybridizations; real-time qPCR; the generation of polyclonal antibodies to HB3var3 NTS-DBLα1, HB3var3 di-domain, and 3D7 PFD0020c NTS-DBLα1; the generation of polyclonal antibodies to HB3var3 DBLδ5 and 3D7 PFD0020c DBLγ6; and flow cytometry with plasma from African children.

Parasite and Human Endothelial Cell Culture. *P. falciparum* strains HB3, 3D7, IT/FCR3, and Dd2 were cultured in supplemented RPMI medium as described (61). The HBEC-5i cell line is an immortalized endothelial line described previously (5). HBEC-5i cells were grown in DMEM/F-12 medium (Sigma) supplemented with 2 mM L-glutamine, endothelial cell growth supplement (5 mL of 100× per 500 mL of medium, hereafter referred as "incomplete medium") (ScienCell), and 10% vol/vol heat-inactivated bovine serum. Parasite strains were selected by panning as described in detail previously (9). For HB3-HBEC-TNF, HBEC-5i cells were activated 24 h before selection by addition of TNFα at 50 μg/mL. HBMEC, HDMEC, and HPMEC (all from ScienCell) were cultured as for HBEC-5i cells, except for the use of endothelial cell medium (ScienCell) and bovine serum at 5% vol/vol, following the manufacturer's instructions.

Binding Assays on Endothelial Cells. The day before the assay, endothelial cells were plated on fibronectin-coated eight-well chamber slides (BioCoat 354628; BD) at 10^4 cells per well. For each assay, at least two replicate wells per slide were used. Parasite cultures were washed twice with incomplete medium. Two hundred microliters of parasite culture (pigmented trophozoites at 5–10% parasitemia and 2% hematocrit) in incomplete DMEM/1% BSA were added per well. The slide was incubated for 75 min at 37 °C with gentle resuspension of cells halfway through the incubation. The chamber then was removed according to the manufacturer's instructions. The slide was washed in a 100-mm Petri dish (351029; BD) filled with incomplete DMEM. The slide was held still using tweezers, and the dish was rocked gently. This step was repeated four times, each time in a new dish with fresh medium. The slide was checked under an inverted microscope to ensure there were no or few unbound cells remaining. It then was fixed and stained with 1% glutaraldehyde for at least 1 h and was stained with 5% vol/vol Giemsa for 20 min. IEs bound to at least 100 isolated cells were counted by light microscopy using the 100× objective. For rebinding assays, after the washing step, bound IEs were detached by flushing the cell surface with incomplete DMEM using a Pasteur

pipette at least 10 times. IEs were placed in a 15-mL tube and centrifuged at 300 × *g* for 5min. They were resuspended with 200 μL of incomplete DMEM per well and then were reincubated on endothelial cells as above.

IFA and Flow Cytometry with Antibodies to PfEMP1. IFA with rabbit preimmune and immune sera and live IEs were carried out as described (23). For each antigen, the rabbit serum giving the brightest IFA signal with the lowest background was chosen for purification of total IgG. Staining for flow cytometry was carried out as for IFA except that all incubations included 1.25 μg/mL Hoechst (instead of DAPI) to stain parasite nuclei. After the secondary incubation (1:1,000 of a highly cross-absorbed Alexa Fluor 488 goat anti-rabbit IgG) (Invitrogen) and washes, cells were fixed in 0.5% paraformaldehyde on ice for 20 min and washed twice in FACS buffer (PBS/0.1% BSA/0.1% sodium azide). Cells were resuspended in 500 μL of FACS buffer and analyzed on a Becton-Dickinson LSRII flow cytometer by counting 500,000 events.

Antibody Inhibition of Binding to HBEC-5i Cells. Binding assays were carried out as described above, with a preincubation step in which the culture suspension (5–10% parasitemia and 2% hematocrit in incomplete DMEM/1% BSA) was incubated for 20 min with antibodies to PfEMP1 or controls (concentrations are shown in figure legends). Two hundred microliters of this suspension were added per well on the endothelial cell culture slide, and the assay was completed as described above. Binding was compared with control wells with no added IgG. All antibodies were tested in at least three independent experiments with at least triplicate wells per antibody in each experiment.

Statistical Analysis. Graphs and statistical analysis were carried out using GraphPad Prism software (GraphPad).

ACKNOWLEDGMENTS. This work was funded by the Wellcome Trust through a 4-y doctoral studentship (to A.C.), a Senior Fellowship in Basic Biomedical Science (to J.A.R), Grant 084226, a Strategic Award (Grant 084538 to C.A.), and Wellcome Trust Programme Grants 084535 and 077092 (to P.C.B.). C.W.W. and L.T. were supported by Danish Medical Research Council Grant 271-08-0540. This paper was submitted with the permission of the director of the Kenya Medical Research Institute.

1. Idro R, Marsh K, John CC, Newton CR (2010) Cerebral malaria: Mechanisms of brain injury and strategies for improved neurocognitive outcome. *Pediatr Res* 68:267–274.
2. van der Heyde HC, Nolan J, Combes V, Gramaglia I, Grau GE (2006) A unified hypothesis for the genesis of cerebral malaria: Sequestration, inflammation and hemostasis leading to microcirculatory dysfunction. *Trends Parasitol* 22:503–508.
3. Mishra SK, Newton CR (2009) Diagnosis and management of the neurological complications of falciparum malaria. *Nat Rev Neurol* 5:189–198.
4. White NJ, Turner GD, Medana IM, Dondorp AM, Day NP (2010) The murine cerebral malaria phenomenon. *Trends Parasitol* 26:11–15.
5. Dorovini-Zis K, Prameya R, Bowman PD (1991) Culture and characterization of microvascular endothelial cells derived from human brain. *Lab Invest* 64:425–436.
6. Xiao L, et al. (1996) *Plasmodium falciparum*: Involvement of additional receptors in the cytoadherence of infected erythrocytes to microvascular endothelial cells. *Exp Parasitol* 84:42–55.
7. Wassmer SC, Cianciolo GJ, Combes V, Grau GE (2005) Inhibition of endothelial activation: A new way to treat cerebral malaria? *PLoS Med* 2:e245.
8. Wassmer SC, Combes V, Candal FJ, Juhan-Vague I, Grau GE (2006) Platelets potentiate brain endothelial alterations induced by *Plasmodium falciparum*. *Infect Immun* 74: 645–653.
9. Claessens A, Rowe JA (2012) Selection of *Plasmodium falciparum* parasites for cytoadhesion to human brain endothelial cells. *J Vis Exp* 59:e3122.
10. Tembo D, Montgomery J (2010) Var gene expression and human *Plasmodium* pathogenesis. *Future Microbiol* 5:801–815.
11. Rowe JA, Claessens A, Corrigan RA, Arman M (2009) Adhesion of *Plasmodium falciparum*-infected erythrocytes to human cells: Molecular mechanisms and therapeutic implications. *Expert Rev Mol Med* 11:e16.
12. Kraemer SM, Smith JD (2006) A family affair: *var* genes, PfEMP1 binding, and malaria disease. *Curr Opin Microbiol* 9:374–380.
13. Smith JD, Subramanian G, Gamain B, Baruch DI, Miller LH (2000) Classification of adhesive domains in the *Plasmodium falciparum* erythrocyte membrane protein 1 family. *Mol Biochem Parasitol* 110:293–310.
14. Robinson BA, Welch TL, Smith JD (2003) Widespread functional specialization of *Plasmodium falciparum* erythrocyte membrane protein 1 family members to bind CD36 analysed across a parasite genome. *Mol Microbiol* 47:1265–1278.
15. Janes JH, et al. (2011) Investigating the host binding signature on the *Plasmodium falciparum* PfEMP1 protein family. *PLoS Pathog* 7:e1002032.
16. Kirchgatter K, Portillo HdelA (2002) Association of severe noncerebral *Plasmodium falciparum* malaria in Brazil with expressed PfEMP1 DBL1 alpha sequences lacking cysteine residues. *Mol Med* 8:16–23.
17. Jensen AT, et al. (2004) *Plasmodium falciparum* associated with severe childhood malaria preferentially expresses PfEMP1 encoded by group A *var* genes. *J Exp Med* 199:1179–1190.
18. Kyriacou HM, et al. (2006) Differential *var* gene transcription in *Plasmodium falciparum* isolates from patients with cerebral malaria compared to hyperparasitaemia. *Mol Biochem Parasitol* 150:211–218.
19. Warimwe GM, et al. (2009) *Plasmodium falciparum* var gene expression is modified by host immunity. *Proc Natl Acad Sci USA* 106:21801–21806.
20. Rowe JA, Moulds JM, Newbold CI, Miller LH (1997) *P. falciparum* rosetting mediated by a parasite-variant erythrocyte membrane protein and complement-receptor 1. *Nature* 388:292–295.
21. Vigan-Womas I, et al. (2008) An in vivo and in vitro model of *Plasmodium falciparum* rosetting and autoagglutination mediated by varO, a group A *var* gene encoding a frequent serotype. *Infect Immun* 76:5565–5580.
22. Vigan-Womas I, et al. (2011) Allelic diversity of the *Plasmodium falciparum* erythrocyte membrane protein 1 entails variant-specific red cell surface epitopes. *PLoS ONE* 6:e16544.
23. Ghumra A, et al. (2011) Immunisation with recombinant PfEMP1 domains elicits functional rosette-inhibiting and phagocytosis-inducing antibodies to *Plasmodium falciparum*. *PLoS ONE* 6:e16414.
24. Ghumra A, et al. (2012) Induction of Strain-Transcending Antibodies Against Group A PfEMP1 Surface Antigens from Virulent Malaria Parasites. *PLoS Pathog* 8:e1002665.
25. Claessens A, et al. (2011) Design of a variant surface antigen-supplemented microarray chip for whole transcriptome analysis of multiple *Plasmodium falciparum* cytoadherent strains, and identification of strain-transcendent *rif* and *stevor* genes. *Malar J* 10:180.
26. Crabb BS, et al. (1997) Targeted gene disruption shows that knobs enable malaria-infected red cells to cytoadhere under physiological shear stress. *Cell* 89:287–296.
27. Seydel KB, Milner DA, Jr., Kamiza SB, Molyneux ME, Taylor TE (2006) The distribution and intensity of parasite sequestration in comatose Malawian children. *J Infect Dis* 194:208–215.
28. Biswas AK, et al. (2007) *Plasmodium falciparum* uses gC1qR/HABP1/p32 as a receptor to bind to vascular endothelium and for platelet-mediated clumping. *PLoS Pathog* 3: 1271–1280.
29. Andrews KT, Adams Y, Viebig NK, Lanzer M, Schwartz-Albiez R (2005) Adherence of *Plasmodium falciparum* infected erythrocytes to CHO-745 cells and inhibition of binding by protein A in the presence of human serum. *Int J Parasitol* 35:1127–1134.
30. Berendt AR, et al. (1992) The binding site on ICAM-1 for *Plasmodium falciparum*-infected erythrocytes overlaps, but is distinct from, the LFA-1-binding site. *Cell* 68: 71–81.
31. Bozdech Z, et al. (2003) The transcriptome of the intraerythrocytic developmental cycle of *Plasmodium falciparum*. *PLoS Biol* 1:E5.
32. Taylor HM, Kyes SA, Harris D, Kriek N, Newbold CI (2000) A study of *var* gene transcription in vitro using universal *var* gene primers. *Mol Biochem Parasitol* 105: 13–23.
33. Bull PC, et al. (2005) *Plasmodium falciparum* variant surface antigen expression patterns during malaria. *PLoS Pathog* 1:e26.
34. Wang CW, Magistrado PA, Nielsen MA, Theander TG, Lavstsen T (2009) Preferential transcription of conserved *rif* genes in two phenotypically distinct *Plasmodium falciparum* parasite lines. *Int J Parasitol* 39:655–664.
35. Kyes SA, Rowe JA, Kriek N, Newbold CI (1999) Rifins: A second family of clonally variant proteins expressed on the surface of red cells infected with *Plasmodium falciparum*. *Proc Natl Acad Sci USA* 96:9333–9338.
36. Llinás M, Bozdech Z, Wong ED, Adai AT, DeRisi JL (2006) Comparative whole genome transcriptome analysis of three *Plasmodium falciparum* strains. *Nucleic Acids Res* 34: 1166–1173.
37. Sargeant TJ, et al. (2006) Lineage-specific expansion of proteins exported to erythrocytes in malaria parasites. *Genome Biol* 7:R12.
38. Pasloske BL, et al. (1993) Cloning and characterization of a *Plasmodium falciparum* gene encoding a novel high-molecular weight host membrane-associated protein, PfEMP3. *Mol Biochem Parasitol* 59:59–72.
39. Brown GV, et al. (1985) Localization of the ring-infected erythrocyte surface antigen (RESA) of *Plasmodium falciparum* in merozoites and ring-infected erythrocytes. *J Exp Med* 162:774–779.
40. Spycher C, et al. (2003) MAHRP-1, a novel *Plasmodium falciparum* histidine-rich protein, binds ferriprotoporphyrin IX and localizes to the Maurer's clefts. *J Biol Chem* 278:35373–35383.
41. Rask TS, Hansen DA, Theander TG, Gorm Pedersen A, Lavstsen T (2010) *Plasmodium falciparum* erythrocyte membrane protein 1 diversity in seven genomes–divide and conquer. *PLOS Comput Biol* 6:e1000933.
42. Cham GK, et al. (2008) A semi-automated multiplex high-throughput assay for measuring IgG antibodies against *Plasmodium falciparum* erythrocyte membrane protein 1 (PfEMP1) domains in small volumes of plasma. *Malar J* 7:108.
43. Avril M, et al. (2012) A restricted subset of *var* genes mediates adherence of *Plasmodium falciparum*-infected erythrocytes to brain endothelial cells. *Proc Natl Acad Sci USA*, 10.1073/pnas.1120534109.
44. Lavstsen T, et al. (2012) *Plasmodium falciparum* erythrocyte membrane protein 1 domain cassettes 8 and 13 are associated with severe malaria in children. *Proc Natl Acad Sci USA*, 10.1073/pnas.1120455109.
45. Tham WH, Payne PD, Brown GV, Rogerson SJ (2007) Identification of basic transcriptional elements required for *rif* gene transcription. *Int J Parasitol* 37:605–615.
46. Spycher C, et al. (2008) The Maurer's cleft protein MAHRP1 is essential for trafficking of PfEMP1 to the surface of *Plasmodium falciparum*-infected erythrocytes. *Mol Microbiol* 68:1300–1314.

47. Mok BW, et al. (2007) Comparative transcriptomal analysis of isogenic *Plasmodium falciparum* clones of distinct antigenic and adhesive phenotypes. *Mol Biochem Parasitol* 151:184–192.
48. Daily JP, et al. (2005) In vivo transcriptome of *Plasmodium falciparum* reveals overexpression of transcripts that encode surface proteins. *J Infect Dis* 191:1196–1203.
49. Eksi S, et al. (2005) Identification of a subtelomeric gene family expressed during the asexual-sexual stage transition in *Plasmodium falciparum*. *Mol Biochem Parasitol* 143: 90–99.
50. Mayer C, Slater L, Erat MC, Konrat R, Vakonakis I (2012) Structural analysis of the *Plasmodium falciparum* erythrocyte membrane protein 1 (PfEMP1) intracellular domain reveals a conserved interaction epitope. *J Biol Chem* 287:7182–7189.
51. Normark J, et al. (2007) PfEMP1-DBL1alpha amino acid motifs in severe disease states of *Plasmodium falciparum* malaria. *Proc Natl Acad Sci USA* 104:15835–15840.
52. Rowe JA, Shafi J, Kai OK, Marsh K, Raza A (2002) Nonimmune IgM, but not IgG binds to the surface of *Plasmodium falciparum*-infected erythrocytes and correlates with rosetting and severe malaria. *Am J Trop Med Hyg* 66:692–699.
53. Ochola LB, et al. (2011) Specific receptor usage in *Plasmodium falciparum* cytoadherence is associated with disease outcome. *PLoS ONE* 6:e14741.
54. Newbold C, et al. (1997) Receptor-specific adhesion and clinical disease in *Plasmodium falciparum*. *Am J Trop Med Hyg* 57:389–398.
55. Rogerson SJ, et al. (1999) Cytoadherence characteristics of *Plasmodium falciparum*-infected erythrocytes from Malawian children with severe and uncomplicated malaria. *Am J Trop Med Hyg* 61:467–472.
56. Heddini A, et al. (2001) Fresh isolates from children with severe *Plasmodium falciparum* malaria bind to multiple receptors. *Infect Immun* 69:5849–5856.
57. Fernandez-Reyes D, et al. (1997) A high frequency African coding polymorphism in the N-terminal domain of ICAM-1 predisposing to cerebral malaria in Kenya. *Hum Mol Genet* 6:1357–1360.
58. Craig A, et al. (2000) A functional analysis of a natural variant of intercellular adhesion molecule-1 (ICAM-1Kilifi). *Hum Mol Genet* 9:525–530.
59. Fry AE, et al. (2008) Variation in the ICAM1 gene is not associated with severe malaria phenotypes. *Genes Immun* 9:462–469.
60. Howell DP, et al. (2008) Mapping a common interaction site used by *Plasmodium falciparum* Duffy binding-like domains to bind diverse host receptors. *Mol Microbiol* 67:78–87.
61. Corrigan RA, Rowe JA (2010) Strain variation in early innate cytokine induction by *Plasmodium falciparum*. *Parasite Immunol* 32:512–527.
62. Kraemer SM, et al. (2007) Patterns of gene recombination shape var gene repertoires in *Plasmodium falciparum*: Comparisons of geographically diverse isolates. *BMC Genomics* 8:45.

Text S1. Supplementary Materials and Methods.

Adhesion properties of selected and unselected parasite lines. The rosette frequency (percentage of IE binding two or more uninfected E) of unselected and HBEC-selected parasite lines was determined by microscopy of ethidium-bromide-stained wet preparations as described (1). The clumping frequency (percentage of IE in clumps of three or more IE in the presence of platelets) was determined by microscopy of ethidium-bromide-stained wet preparations (2) with the clumping assay set up at 1% parasitaemia, 10% haematocrit with 20% platelet-rich plasma and incubated for 60 mins at 10 rpm. Spot binding assays were as described (3) with proteins/concentrations as shown in Table S1 (SI Appendix). The IFA for Knobs was carried out on thin smears fixed with 90% acetone/10% methanol and incubated with 10 μg/ml of mAb 89 to KAHRP (4) or IgG2a isotype control for 1h, followed by 3x washes in PBS and secondary incubation for 45 mins with 1/500 dilution of highly cross-absorbed Alexa Fluor 488 goat anti-mouse IgG with 1 μg/ml of DAPI to stain parasite nuclei. After 3x further washed the slides were mounted with Fluoromount and viewed by fluorescence microscopy. 100 IEs were counted for presence/absence of knobs in four separate areas of each slide to give the mean knob positivity and SEM for each strain.

Microarray hybridizations. HBEC-selected parasites were cultured and synchronized alongside their unselected (non-binding) counterpart. At late schizont stage, HB3-HBEC1 and HB3-Uns1 control cultures (pilot experiment) were Percoll-treated to purify IEs (5), while for all other selections, schizont-IEs were purified on a MACS column (6). Five to seven hours later, after most schizonts had ruptured and parasites were mostly at early-ring stage, cultures were sorbitol-treated (7). Time point 1 of a time-course experiment started 8 hours after the end of the Percoll/MACS

treatment (i.e. 1-3 hours after sorbitol treatment). Samples were processed as described previously (8). Briefly, after RNA extraction, a reference pool was created from each unselected strain by pooling an equal amount of RNA from each time point. After reverse-transcription, each time point sample (from selected and unselected populations) was labelled with Cy5 (red) while the reference pool was labelled with Cy3 (green). Samples were then hybridized overnight. The exception to this was a pilot experiment in which each HB3-HBEC1 time point was hybridised directly with HB3-Uns1 time points rather than using a reference pool.

Microarray data were analysed as described (8). Briefly, each array was normalized with Lowess. Only spots with median intensities greater than the local background plus 2 times the standard deviation of the background were used. For data visualisation, the [HBEC-selected/pool] ratios were divided by the [unselected/pool] ratios to obtain [HBEC-selected/unselected] ratios. Data for HB3-HBEC-2 time point 6 is missing due to a technical problem. Data analysis was carried out using Microsoft Excel, MeV (9), Cluster (http://bonsai.ims.utokyo.ac.jp/~mdehoon/software/cluster/software.htm#ctv) and Jalview (http://jtreeview.sourceforge.net/) for data visualization. All microarray data have been deposited in the GEO repository (GSE32211): http://www.ncbi.nlm.nih.gov/geo/query/acc.cgi?acc=GSE32211

Real-Time Quantitative (q)PCR. Transcript levels of the *var* genes from 3D7, IT/FCR3 and HB3 parasite strains and the *rif* genes located head-to-head with the group A *var* gene candidate ligands were determined by real-time qPCR performed on a Rotorgene RG-3000 thermal cycler (Corbett Research) as previously described (10, 11). Primers designed to amplify the *rif* genes of the HB3 strain were as follows: PFHG_03235: forward-tgcgaaaagtcgatagcaga, reverse-agccgctttagtagcagcag; PFHG

_03841: forward-catagtgatgccattccaacat, reverse-ccacctattaatcccaattctgg; PFHG _05051/HB3RifA_081: forward-actgtgggtatgggttaggaagt, reverse-gctttagcaataccttcctggat; PFHG _03670: forward-agtgctatgcccgacaattt, reverse-acaccggttttagcatcagc; PFHG _02275: forward-gatatgttgacataccttcctggt, reverse-agcgtttgaagaattgcaca. Transcript level differences between selected and unselected parasite lines were calculated as ΔΔCt-values and shown as fold changes ($2^{\Delta\Delta Ct}$) (User Bulletin #2: ABI Prism 7700 Sequence Detection System; http://www3.appliedbiosystems.com/cms/groups/mcb_support/documents/generaldocuments/cms_040980.pdf, Applied Biosystems).

Generation of polyclonal antibodies to HB3var3 NTS-DBLα1, HB3var3 di-domain and 3D7 PFD0020c NTS-DBLα1. Recombinant PfEMP1 domains were produced in *E. coli* and purified as described previously (12). The domain boundaries for HB3var3 NTS-DBLα1 were Met1-Pro468, for HB3var3 di-domain were Met1-Arg762 and for 3D7 PFD0020c NTS-DBLα1 were Met1-Pro475. Primers were as follows: HB3var3 NTS-DBLα1 and di-domain forward 5'-aaggatccatggggtcaagcgcatcaaaa-3'; HB3var3 NTS-DBLα1 reverse 5'-aagctagcttatggacatacttggcaataatc-3'; HB3var3 di-domain reverse 5'-aagctagcttagcgctcattcaattgtttgtg-3'; 3D7 PFD0020c forward 5'-aaggatccatggggacaggttcatcaact-3' and reverse 5'-ttgctagcttagggacagggttggcaataatc. Purified proteins with the his-tag removed by TEV protease cleavage (12) were used to immunize rabbits (two per antigen). The rabbits were pre-screened by IFA to exclude animals with heterophilic antibodies that recognise either infected or uninfected Es as described previously (12). All immunizations were carried out by BioGenes GmbH (Berlin, Germany). Rabbits were immunized with 125 μg of protein

on days 0, 7, 14 and 28. An ELISA 50% end titre of at least 1:25,000 was observed for each anti-serum (BioGenes GmbH).

Generation of polyclonal antibodies to HB3var3 DBLδ5 and 3D7 PFD0020c DBLγ6. The HB3var3 DBLδ5 domain was amplified from HB3 genomic DNA by primers LT510 5'-ggatccctgtgaaatcgtggataaaacactgg-3' and LT511 5'-ctgcggccgctacatggagcacagtattctgcatg-3'. The PFD0020c DBLγ6 domain was amplified from 3D7 genomic DNA by primers LT23 5′-cggatccc tgtaatggaattaagacacttcttg-3′and LT24 5′-tgcggccgctcgcactttgtgttggtgctg-3′. The products were cloned and expressed in a baculovirus/insect cell system and recombinant protein purified on a nickel affinity column as described (13). Rabbit antiserum was raised by subcutaneous injection of 10-20 μg protein in complete Freund's adjuvant followed by two boosters of protein in incomplete Freund's adjuvant. Recombinant GammaBind^{TM} G type 2 coupled to Sepharose^{TM} 4B (GE Healthcare) was used to purify IgG according to the manufacturer's instructions.

Flow cytometry with plasma from African children. Isogenic pairs of unselected and HBEC-selected parasites were frozen as trophozoites (14) at 1% parasitaemia. Plasma samples were collected from children attending Kilifi District Hospital between 2006-2010. Ethical approval was granted by the KEMRI Ethical Review Committee (SSC protocol number 1131) and informed consent obtained from the participants parents/guardians. Plasma samples from 10 children admitted with cerebral malaria (*P. falciparum* parasitaemia, fever and Blantyre coma score of ≤2 with other causes of coma excluded) were tested along with their age, blood group and date of admission-matched uncomplicated malaria controls (children seen in outpatients or admitted but with no signs of severe malaria). Acute plasma samples were collected at the time of admission to hospital and convalescent samples collected

3-4 weeks later. Flow cytometry was as described (15). Briefly, 11.5µl of ethidium bromide-stained (10µg/ml) parasite culture suspension (2% haematocrit in PBS/0.5% BSA) was incubated with 1µl test plasma in 96-well U-bottomed plates (Falcon, Becton Dickinson, USA) for 30 mins at room temperature (RT). The cells were washed three times with 200µl of PBS/0.5 % BSA by centrifuging at 1000rpm for 3 mins in a Rotanta 460R centrifuge (Hettich Zentrifugen, Germany). 50µl of FITC-conjugated sheep anti-human IgG-Fc (Binding Site, UK) at a 1:50 dilution in PBS/0.5% BSA was added and incubated for 30 mins at RT in the dark. Following three further washes, the cells were re-suspended in 200µl of PBS/0.5% BSA and 1000 trophozoite-IEs acquired from each well on an FC500 flow cytometer (Beckman Coulter, UK). Analysis was done using Flowjo version 7.6.4.

References

1. Deans AM & Rowe JA (2006) *Plasmodium falciparum*: Rosettes do not protect merozoites from invasion-inhibitory antibodies. Exp Parasitol 112:269-273.
2. Arman M & Rowe JA (2008) Experimental conditions affect the outcome of *Plasmodium falciparum* platelet-mediated clumping assays. Malar J 7:243.
3. Newbold C*, et al.* (1997) Receptor-specific adhesion and clinical disease in *Plasmodium falciparum*. Am J Trop Med Hyg 57:389-398.
4. Taylor DW*, et al.* (1987) Localization of *Plasmodium falciparum* histidine-rich protein 1 in the erythrocyte skeleton under knobs. Mol Biochem Parasitol 25:165-174.
5. Handunnetti SM*, et al.* (1992) Purification and in vitro selection of rosette-positive (R+) and rosette-negative (R-) phenotypes of knob-positive *Plasmodium falciparum* parasites. Am J Trop Med Hyg 46:371-381.
6. Staalsoe T*, et al.* (2003) In vitro selection of *Plasmodium falciparum* 3D7 for expression of variant surface antigens associated with severe malaria in African children. Parasite Immunol 25:421-427.
7. Lambros C & Vanderberg JP (1979) Synchronisation of *Plasmodium falciparum* erythrocytic stages in culture. J Parasitol 65:418-420.
8. Claessens A*, et al.* (2011) Design of a variant surface antigen-supplemented microarray chip for whole transcriptome analysis of multiple *Plasmodium falciparum* cytoadherent strains, and identification of strain-transcendent *rif* and *stevor* genes. Malar J 10:180.
9. Saeed AI*, et al.* (2006) TM4 microarray software suite. Methods Enzymol 411:134-193.
10. Wang CW, Magistrado PA, Nielsen MA, Theander TG, & Lavstsen T (2009) Preferential transcription of conserved *rif* genes in two phenotypically distinct *Plasmodium falciparum* parasite lines. Int J Parasitol 39:655-664.
11. Soerli J*, et al.* (2009) Human monoclonal IgG selection of *Plasmodium falciparum* for the expression of placental malaria-specific variant surface antigens. Parasite Immunol 31:341-346.

12. Ghumra A, *et al.* (2011) Immunisation with recombinant PfEMP1 domains elicits functional rosette-inhibiting and phagocytosis-inducing antibodies to *Plasmodium falciparum*. PLoS ONE 6:e16414.
13. Cham GK, *et al.* (2008) A semi-automated multiplex high-throughput assay for measuring IgG antibodies against *Plasmodium falciparum* erythrocyte membrane protein 1 (PfEMP1) domains in small volumes of plasma. Malar J 7:108.
14. Kinyanjui SM, *et al.* (2004) The use of cryopreserved mature trophozoites in assessing antibody recognition of variant surface antigens of *Plasmodium falciparum*-infected erythrocytes. J Immunol Methods 288:9-18.
15. Bejon P, *et al.* (2009) Analysis of immunity to febrile malaria in children that distinguishes immunity from lack of exposure. Infect Immun 77:1917-1923.

Table S1. Proteins, biomolecules and antibodies used in binding assays.

Protein/molecule/ antibody	Supplier/order number	Type	Diluted in	Concentra-tion used
CD36[a]	R&D Systems: 1955-CD	Recombinant	PBS	25 μg/ml
Chondroitin sulfate A (CSA)[b]	Sigma: C8919	Bovine trachea	PBS	100 μg/ml
E-selectin (CD62E)[c]	R&D Systems: 724-ES	Recombinant	PBS	40 μg/ml
Fibronectin[d]	BD: 354008	Human plasma	BTC[q]	200 μg/ml
Fibronectin	Sigma: F1141	Bovine plasma	BTC[q]	200 μg/ml
Fractalkine/CX3CL1[e]	R&D Systems: 365-FR	Recombinant	PBS	50 μg/ml
gC1qR/HABP1[f]	R&D Systems: 4529-HB	Mouse	PBS	40 μg/ml
Heparan Sulfate Proteoglycan[g]	Sigma: H4777	Purified	PBS	100 μg/ml
Heparin sodium salt	Sigma: H4784	Porcine intestinal mucosa	50mM Tris	50 μg/ml
Hyaluronic acid[h]	Sigma: H1504	Human umbilical cord	2mM $CaCl_2$	100 μg/ml
ICAM1 (CD54)[i]	R&D Systems: 720-IC	Recombinant	PBS	50 μg/ml
Integrin αV β1	Chemicon : CC1092	Purified	PBS	25 μg/ml
Integrin αV β3[j] **(CD51)**	Chemicon : CC1020	Purified	PBS	25 μg/ml
NCAM (CD56)[k]	Chemicon: AG265	Embryonic chicken brain	PBS	10 μg/ml
PECAM-1 (CD31)[l]	R&D Systems: ADP6	Recombinant	PBS	50 μg/ml
P-Selectin (CD62P)[m]	R&D Systems: 137-PS	Recombinant	PBS	40 μg/ml
Thrombospondin[n]	Calbiochem: 605225	Purified	50mM Tris	50 μg/ml
VCAM-1 (CD106)[c]	R&D Systems: 862-VC	Recombinant	PBS	50 μg/ml
CD36 antibody FA6-152[o]	Beckman Coulter IM2279U	Mouse IgG1 mAb	PBS	10 μg/ml
ICAM-1 antibody 15.2[p]	AbD Serotec MCA1615XZ	Mouse IgG1 mAb	PBS	20 μg/ml
ICAM-1 antibody 15.8	Gift from Prof Alister Craig	Mouse IgG1 mAb	PBS	20 μg/ml

[a] Reference (1, 2)

[b] Reference (3)

[c] Reference (4)

[d] Reference (5)

[e] Reference (6)

[f] Reference (7)

[g] Reference (8)

[h] Reference (9)

[i] Reference (10). Integrin αVβ1 was included as a negative control.

[j] Reference (11)

[k]Reference (12). NCAM was incubated for 2 hours at 37°C with 1U/ml Neuraminidase (Sigma N3001) to digest polysialic acid (PSA) (12).

[l] Reference (13)

[m] Reference (14)

[n] Reference (15)

[o] Reference (16)

[p] Reference (17)

[q] BTC = 50mM Bis-Tris, 100mM NaCl, 25 mM Calcium lactate, 1 mM $MnCl_2$, pH7.4.

References

1. Oquendo P, Hundt E, Lawler J, & Seed B (1989) CD36 directly mediates cytoadherence of *Plasmodium falciparum* parasitized erythrocytes. Cell 58:95-101.
2. Barnwell JW*, et al.* (1989) A human 88-kD membrane glycoprotein (CD36) functions in vitro as a receptor for a cytoadherence ligand on *Plasmodium falciparum*-infected erythrocytes. J Clin Invest 84:765-772.
3. Fried M & Duffy PE (1996) Adherence of *Plasmodium falciparum* to chondroitin sulphate A in the human placenta. Science 272:1502-1504.
4. Ockenhouse CF*, et al.* (1992) Human vascular endothelial cell adhesion receptors for *Plasmodium falciparum*-infected erythrocytes: roles for endothelial leukocyte adhesion molecule 1 and vascular cell adhesion molecule 1. J Exp Med 176:1183-1189.
5. Eda S & Sherman IW (2004) *Plasmodium falciparum*-infected erythrocytes bind to the RGD motif of fibronectin via the band 3-related adhesin. Exp Parasitol 107:157-162.

6. Hatabu T, Kawazu S, Aikawa M, & Kano S (2003) Binding of *Plasmodium falciparum*-infected erythrocytes to the membrane-bound form of Fractalkine/CX3CL1. Proc Natl Acad Sci U S A 100:15942-15946.
7. Biswas AK*, et al.* (2007) *Plasmodium falciparum* uses gC1qR/HABP1/p32 as a receptor to bind to vascular endothelium and for platelet-mediated clumping. PLoS Pathog 3:1271-1280.
8. Vogt AM*, et al.* (2003) Heparan sulfate on endothelial cells mediates the binding of *Plasmodium falciparum*-infected erythrocytes via the DBL1alpha domain of PfEMP1. Blood 101:2405-2411.
9. Beeson JG*, et al.* (2000) Adhesion of *Plasmodium falciparum*-infected erythrocytes to hyaluronic acid in placental malaria. Nat Med 6:86-90.
10. Berendt AR, Simmons DL, Tansey J, Newbold CI, & Marsh K (1989) Intercellular adhesion molecule-1 is an endothelial cell adhesion receptor for *Plasmodium falciparum*. Nature 341:57-59.
11. Siano JP, Grady KK, Millet P, & Wick TM (1998) Short report: *Plasmodium falciparum*: cytoadherence to alpha(v)beta3 on human microvascular endothelial cells. Am J Trop Med Hyg 59:77-79.
12. Pouvelle B*, et al.* (2007) Neural cell adhesion molecule, a new cytoadhesion receptor for *Plasmodium falciparum*-infected erythrocytes capable of aggregation. Infect Immun 75:3516-3522.
13. Treutiger CJ, Heddini A, Fernandez V, Muller WA, & Wahlgren M (1997) PECAM-1/CD31, an endothelial receptor for binding *Plasmodium falciparum*-infected erythrocytes. Nat Med 3:1405-1408.
14. Yipp BG*, et al.* (2007) Differential roles of CD36, ICAM-1, and P-selectin in *Plasmodium falciparum* cytoadherence in vivo. Microcirculation 14:593-602.
15. Roberts DD*, et al.* (1985) Thrombospondin binds falciparum malaria parasitized erythrocytes and may mediate cytoadherence. Nature 318:64-66.
16. Andrews KT, Adams Y, Viebig NK, Lanzer M, & Schwartz-Albiez R (2005) Adherence of *Plasmodium falciparum* infected erythrocytes to CHO-745 cells and inhibition of binding by protein A in the presence of human serum. Int J Parasitol 35:1127-1134.
17. Berendt AR*, et al.* (1992) The binding site on ICAM-1 for *Plasmodium falciparum*-infected erythrocytes overlaps, but is distinct from, the LFA-1-binding site. Cell 68:71-81.

Table S2. Summary of selection and synchronisation methods for time-course experiments.

	HB3-HBEC1	HB3-Uns1	HB3-HBEC2	HB3-HBEC TNF[e]	HB3-Uns2	3D7-HBEC	3D7-Uns	IT-HBEC	IT-Uns	Dd2
Rounds of selection[a]	5	/	5	6	/	7	/	6	/	5[f]
Synchronization method[b]	P + S	P + S	M + S	M + S	M + S	M + S	M + S	M + S	M + S	/
Synchronization window[c]	5 hours	5 hours	7 hours	7 hours	6 hours	7 hours	7 hours	7 hours	5 hours	/
Time between last selection and time-course[d]	13 days	/	12 days	12 days	/	14 days	/	13 days	/	/

[a]Number of rounds of selection on HBEC-5i before the time-course.

[b]P = Percoll, S = Sorbitol, M = MACS. See methods section for details.

[c]Time between the end of MACS treatment and the Sorbitol treatment. The shorter the time, the more tightly synchronised the parasites are.

[d]Number of days elapsed between the last round of selection and the start of the time-course.

[e]HB3 parasites selected on HBEC-5i activated with TNF.

[f]The *P. falciparum* Dd2 strain did not increase its binding ability even after 5 rounds of selection on HBEC-5i.

Table S3. Functional enrichment analysis of down-regulated genes

	Pathway Name	# in Genome	# in Input	# in Pathway	# in Input & Pathway	Direction of deviation from expected	Hypergeometric (to be preferred)	Binomial	Gene List
KEGG pathway testing *	Metabolic pathways	5400	290	259	1	UNDER-representation (expect 13, observe 1)	0.00061	0.00372	PFI1110w
GO pathway testing *	GO:0044267|cellular protein metabolic process	5400	290	759	11	UNDER-representation (expect 40, observe 11)	0	0.00001	MAL8P1.70, PFE0370c, PF07_0043, PFD1175w, PFL1885c, PFI0180w, MAL13P1.260, PFL0190w, PFB0665w, PF14_0224, PF14_0027
	GO:0051701|interaction with host	5400	290	8	4	over-representation (expect 0, observe 4)	0.00048	0.00099	PF13_0197, PF10_0345, PF10_0346, PF11_0344
	GO:0030554|adenyl nucleotide binding	5400	290	368	5	UNDER-representation (expect 19, observe 5)	0.00222	0.00292	PF07_0104, PFD1175w, PFL1885c, PF13_0233, PFB0665w
	GO:0016301|kinase activity	5400	290	292	3	UNDER-representation (expect 15, observe 3)	0.00366	0.00469	PFD1175w, PFL1885c, PFB0665w
	GO:0004175|endopeptidase activity	5400	290	188	3	UNDER-representation (expect 10, observe 3)	0.03094	0.03561	MAL8P1.70, PFE0370c, MAL13P1.260
	GO:0016818|hydrolase activity, acting on acid anhydrides, in phosphorus-containing anhydrides	5400	290	165	1	UNDER-representation (expect 8, observe 1)	0.03181	0.03604	PFI0180w
MPM pathway testing*	Functional annotation of merozoite invasion-related proteins	5400	290	60	15	over-representation (expect 3, observe 15)	0	0	PF10_0352, MAL13P1.60, PF10_0351, PF13_0197, PF10_0343, PFL2520w, PFB0570w, PF10_0345, PF10_0281, PFC0110w, PFD1150c, PF10_0346, MAL7P1.176, PF11_0344, PFA0125c
	Subcellular localization of proteins involved in invasion	5400	290	67	12	over-representation (expect 3, observe 12)	0.00019	0.00033	MAL13P1.60, PF10_0351, PF13_0197, PF10_0343, PFL2520w, PF10_0345, PFC0110w, PFD1150c, PF10_0346, MAL7P1.176, PF11_0344, PFA0125c
Testing for Transcription factor*	Transcription Factor								No Transcription Factor(s) are significantly enriched

KEGG: Kyoto Encyclopedia of Genes and Gernomes; GO: Gene Ontology; MPM: Malaria Metabolic Pathway. *(level for statistical significance = 0.05)

Table S4. Pair-wise amino acid identities for HBEC-binding variants (whole protein, extracellular domain, NTS-DBLα, CIDR1, DBLδ and CIDR2)

	HB3var3	ITvar7	ITvar19	PFD0020c
Pair-wise amino acid identities for whole protein				
HB3var3	100	36.2	32.5	34.4
ITvar7		100	33.6	45.7
ITvar19			100	41.9
PFD0020c				100
Pair-wise amino acid identities for extracellular domain encoded by exon 1				
HB3var3	100	34.8	29.6	32.8
ITvar7		100	28.5	39.3
ITvar19			100	37.9
PFD0020c				100
Pair-wise amino acid identities for NTS-DBLα				
HB3var3	100	58.1	42.9	49.5
ITvar7		100	45.9	52.1
ITvar19			100	46.5
PFD0020c				100
Pair-wise amino acid identities for CIDR1				
HB3var3	100	74.4	39.2	40.6
ITvar7		100	42.8	40.2
ITvar19			100	74.2
PFD0020c				100
Pair-wise amino acid identities for DBLδ				
HB3var3	100	36.8	37.7	37.9
ITvar7		100	45.4	48.4
ITvar19			100	47.0
PFD0020c				100
Pair-wise amino acid identities for CIDR2				
HB3var3	100	38.9	42.0	24.2
ITvar7		100	47.8	22.3
ITvar19			100	26.5
PFD0020c				100

Table S5. Pair-wise amino acid identities for DBLβ and DBLγ from HBEC-binding variants

Pair-wise amino acid identities for DBLβ from HBEC-binding variants						
	HB3var3 d2[a]	HB3var3 d5[b]	ITvar7 d2[a]	ITvar7 d3[c]	ITvar19	PFD0020c
HB3var3 d2[a]	100	44.1	52.2	46.4	49.2	49.4
HB3var3 d5[b]		100	41.4	51.0	46.0	47.1
ITvar7 d2[a]			100	45.2	50.2	47.2
ITvar7 d3[c]				100	47.8	46.8
ITvar19					100	58.5
PFD0020c						100
Pair-wise amino acid identities for DBLγ from HBEC-binding variants						
	HB3var3	ITvar7	ITvar19 d3[c]	ITvar19 d5[b]	PFD0020c d3[c]	PFD0020c d4[d]
HB3var3	100	45.0	49.3	38.7	45.6	47.4
ITvar7		100	33.0	42.7	36.0	56.2
ITvar19 d3[c]			100	36.3	52.6	38.9
ITvar19 d5[b]				100	35.7	44.4
PFD0020c d3[c]					100	39.2
PFD0020c d4[d]						100

[a]d2: 2nd DBL domain from the N-terminus
[b]d5: 5th DBL domain from the N-terminus
[c]d3: 3rd DBL domain from the N-terminus
[d]d4: 4th DBL domain from the N-terminus

Supplementary Figure legends.

Figure S1. Adhesion properties of HBEC-selected parasite lines.

A) The rosette frequency (percentage of IE binding two or more uninfected E) of unselected and HBEC-selected parasite lines was determined by microscopy of ethidium-bromide-stained wet preparations as described (1). The experiment was performed twice for HB3-Uns and HB3-HBEC, once for all other strains. B) The clumping frequency (percentage of IE in clumps of three or more IE in the presence of platelets) was determined by microscopy of ethidium-bromide-stained wet preparations as described (2). The clumping assay was set up at 1% Pt, 10% Ht with 20% platelet-rich plasma and incubated for 60 mins. Data shown are mean and SD from three independent experiments for each strain. There was a significant drop in the clumping frequency after selection for HBEC-binding in all strains (** $p<0.01$ for each strain, paired t test). C) Spot binding assays with HB3 parasite lines. Three µl spots of soluble receptors in PBS were absorbed overnight onto Falcon 351007 plates. The source and concentration of each molecule is shown in Table S1. Spots were removed by suction and the plates blocked with PBS/2% BSA for two hours. Parasite culture suspension in RPMI binding medium (BM)/1% BSA pH 7.1 at 2% Ht, 5% Pt was incubated with the plates for 1 hour, with gentle resuspension every 12 minutes. Plates were washed gently with BM to remove unbound cells. Bound cells were fixed with 1% glutaraldehyde for 1 hour and stained with 5% Giemsa for 20 mins. The number of adherent IEs were counted in at least five fields of each a spot viewed with the 100x objective. PBS was always used as a negative control, CD36 as a positive control. Data shown are the mean and SD from at

least two independent assays, with each assay comprising at least 3 spots for each molecule per plate, and at least two plates. Statistically significant differences between Uns- and HBEC-selected parasites are shown *p<0.05 ** p<0.01, ***p<0.001. D) Spot binding assays with IT parasite lines as for part C. E) Binding inhibition assay of HB3-HBEC parasites on HBEC-5i in the presence of antibodies known to block adhesion to ICAM-1 (15.2 and 15.8) and CD36 (FA6-152). Data shown are the mean and SD from two independent experiments, with at least two wells per antibody in each experiment.

Figure S2. Parasite maturity during the HB3 time-course. Parasites were synchronized as described in the methods/Table S1 to give a five-hour time window. The first sample was collected 3 hours after sorbitol lysis, and samples were then taken 8-hourly throughout the asexual blood stage cycle. The maximum parasite maturity in terms of hours post invasion at each time point is shown in the second column. Samples for RNA extraction were taken from the culture at each time point, mixed with TRIzol reagent and frozen, and a Giemsa-stained thin blood smear was performed to record the developmental stage of the selected and unselected parasites.

Figure S3. Pearson correlation of time points between selected and unselected parasite strains. Gene transcription data from all oligonucleotide probes from one time point in an unselected strain were correlated with data from all oligonucleotide probes of one time point of the selected strain. A Pearson correlation close to 1 shows a strong positive correlation and a value close to -1 shows a strong negative correlation. Here, in almost all cases, the same time point in an unselected strain showed a strong positive

correlation with the same time point in the selected strain (fields with grey background). The largest disparity was found in time point 3 between HB3-HBEC-TNF and HB3-Uns2 (Pearson correlation coefficient 0.34). Gene expression for that time point should therefore be interpreted cautiously. Time point 6 in the IT strain also showed a relatively weak positive correlation (Pearson correlation coefficient 0.51). All other time points and strains showed a strong positive correlation with correlation coefficients of 0.72 or greater, with many being greater than 0.9.

Figure S4. *Var* gene expression profiles determined by reverse transcriptase-PCR in unselected (Uns) and selected (HBEC) parasites. The pie charts represent the frequency of DBLα *var* gene sequence tags detected in each parasite population by reverse transcriptase-PCR with universal primers to DBLα of PfEMP1 (3, 4). 25 to 45 recombinant plasmids containing *var* gene inserts were sequenced for each strain. A) In HB3-HBEC1 and B) HB3-HBEC-TNF, the frequency of *HB3var3* was increased by 14 and 10 fold respectively in selected compared to unselected HB3 ($p < 0.005$, Fisher's exact test). C) The frequency of *PFD0020c* was increased by 16 fold after selection of 3D7 parasites ($p < 0.0001$, Fisher's exact test). D) In IT-HBEC, *ITvar7* was increased nine fold after selection ($p = 0.0184$, Fisher's exact test) while *ITvar19* was detected in 13/45 sequence tags from IT-HBEC in comparison to 0/38 tags from unselected IT ($p = 0.0001$, Fisher's exact test). E) In HB3 selected four times on HDMEC, the frequency of *HB3var3* increased 11-fold after selection ($p = 0.0015$, Fisher's exact test), while for HB3 selected four times on HPMEC, the frequency of *HB3var3* increased nine-fold ($p = 0.0062$, Fisher's exact test). Colour scheme for *var* subgroups: group A genes are in red,

group B in green, group C in blue. Note that *ITvar19*, a group B *var* gene but with group A-like features, is in orange. Nomenclature: A1T= a *var* gene with the A1 upstream sequence found near the telomeres; C1C= a *var* gene with the C1 upstream sequence found near the centromere. T, telomeric; ST, sub-telomeric; C, centromeric; p, pseudogene.

Figure S5. *Rif* and *stevor* genes upregulated in 3D7- and IT-HBEC selected parasites. A) 3D7 *rif* genes (top of panel) and *stevor* genes (bottom of panel) up-regulated by at least three fold in selected parasites. B) IT *rif* genes (top of panel) and *stevor* genes (bottom of panel) up-regulated by at least three fold in selected parasites. Because of the small size of *rif* genes (1-2 kbp) there was only one oligonucleotide probe per gene on the microarray chip. Colour scale as in main text Fig 2.

Figure S6. 15 genes upregulated in selected parasites in at least one time point by two fold or more in all five selections. Data for each gene represents the average of all available oligonucleotide probes. The top 7 genes are proven or predicted to be exported. "ExportPred" = Export prediction score (5). A score of 4.3 or above corresponds to a 95% chance of the protein to be exported. *PF14_0752* (PHISTa) is the only gene to be upregulated by 3 fold in all selections. t, truncated; p, pseudogene. Colour scale as in main text Fig 2.

Figure S7. 58 genes downregulated in selected parasites in at least one time point by two fold or more in all five selections. Data for each gene represents the average of all available oligonucleotide probes. The gene annotation is according to PlasmoDB 6.4. The annotation "INVASION" or "invasion" was added in order to distinguish proteins proven or predicted to be involved in invasion, respectively (6, 7). The top 11 genes are downregulated by at least 3 fold in one or more time point. Colour scale as in main text Fig 2.

Figure S8. Recognition of HBEC-selected and unselected parasites lines by antibodies from African malaria patients. Convalescent plasma samples were collected from 10 cerebral malaria (CM) patients and 10 age- and time of admission-matched uncomplicated malaria patients (UM or uncomp). Surface recognition of HBEC-selected (HBEC) and unselected (uns) parasite lines was tested by flow cytometry. The mean fluorescence intensity (MFI) of the uninfected E population was subtracted from the MFI of the IE population to give the specific MFI of the IE population shown on the y axis. Each data point represents plasma from one patient. A) 3D7 parasites. B) HB3 parasites. C) IT parasites. D) Summary of median MFI, InterQuartile Range (IQR) and P value from Mann Whitney test for all parasite strains.

References.

1. Deans AM & Rowe JA (2006) *Plasmodium falciparum*: Rosettes do not protect merozoites from invasion-inhibitory antibodies. Exp Parasitol 112:269-273.

2. Arman M & Rowe JA (2008) Experimental conditions affect the outcome of *Plasmodium falciparum* platelet-mediated clumping assays. Malar J 7:243.
3. Taylor HM, Kyes SA, Harris D, Kriek N, & Newbold CI (2000) A study of *var* gene transcription in vitro using universal *var* gene primers. Mol Biochem Parasitol 105:13-23.
4. Kyriacou HM*, et al.* (2006) Differential *var* gene transcription in *Plasmodium falciparum* isolates from patients with cerebral malaria compared to hyperparasitaemia. Mol Biochem Parasitol 150:211-218.
5. Sargeant TJ*, et al.* (2006) Lineage-specific expansion of proteins exported to erythrocytes in malaria parasites. Genome Biol 7:R12.
6. Hu G*, et al.* (2010) Transcriptional profiling of growth perturbations of the human malaria parasite *Plasmodium falciparum.* Nat Biotechnol 28:91-98.
7. Haase S*, et al.* (2008) Characterization of a conserved rhoptry-associated leucine zipper-like protein in the malaria parasite *Plasmodium falciparum.* Infect Immun 76:879-887.

A

Unselected parasites	Rosette frequency	HBEC-selected parasites	Rosette frequency
HB3-Uns	<1%	HB3-HBEC	<1%
HB3-Uns2	<1%	HB3-HBEC-TNF	<1%
3D7-Uns	<1%	3D7-HBEC	<1%
IT-Uns	<1%	IT-HBEC	<1%

B

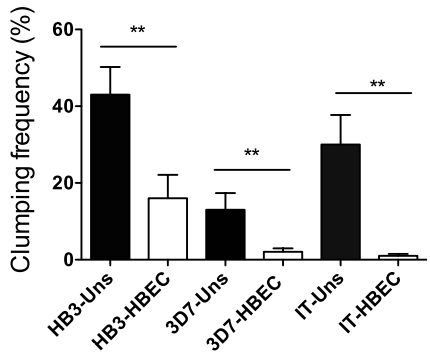

C

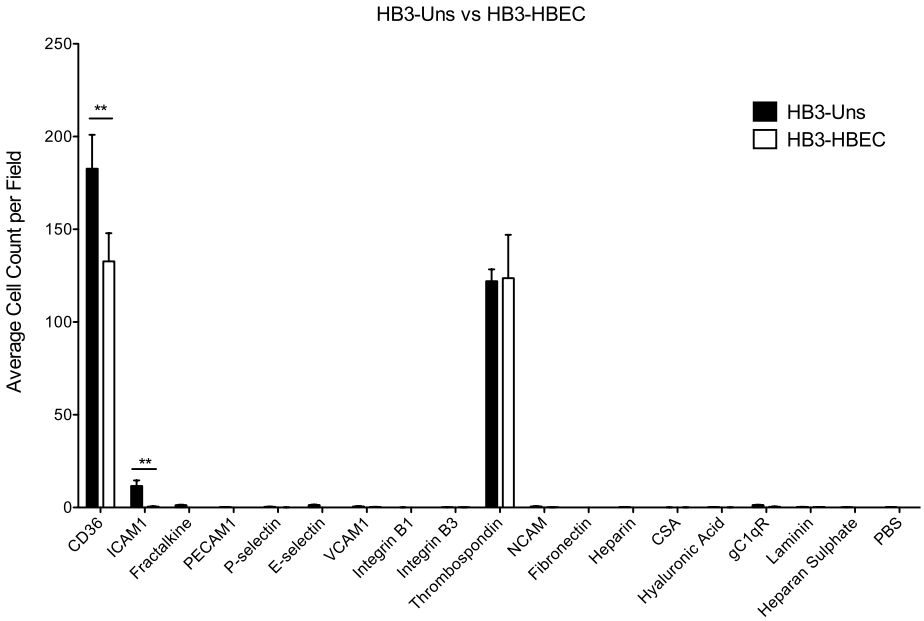

D

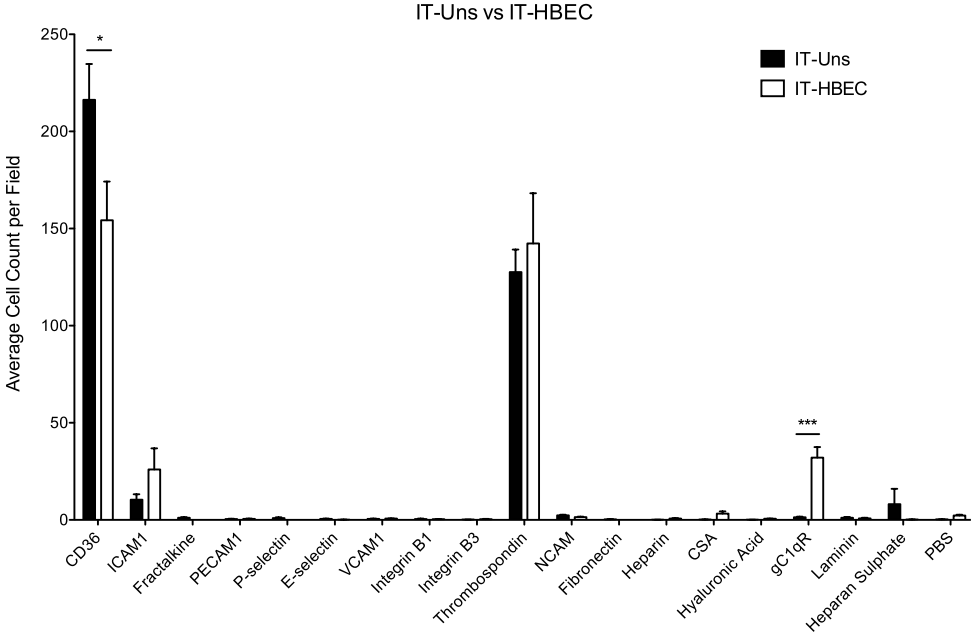

E

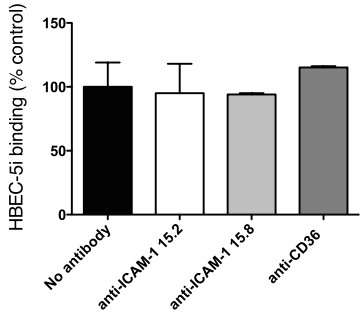

Figure S1

Time-point	Time post invasion	HB3 Unselected	HB3-HBEC Selected
T1 Early ring	8h (range: 3-8h)	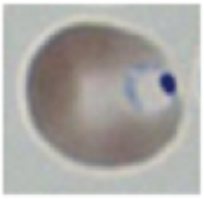	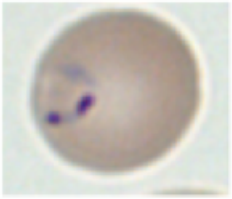
T2 Ring	16h (range: 11-16h)		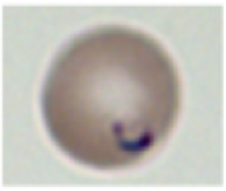
T3 Late ring/early troph	24h (range: 19-24h)	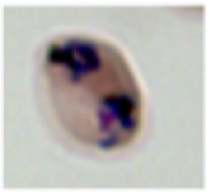	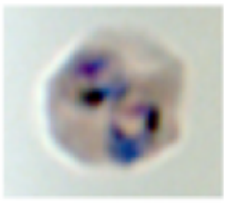
T4 Troph	32h (range: 27-32h)	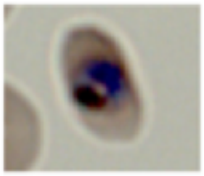	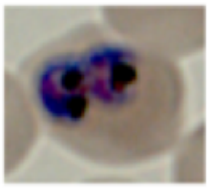
T5 Schizont	40h (range: 35-40h)	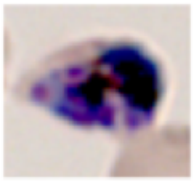	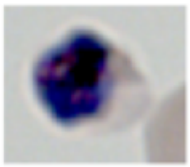
T6 Mature schizont	48h (range: 43-48h)		

Figure S2

		HB3-Uns2					
		T1	**T2**	**T3**	**T4**	**T5**	**T6**
HB3-HBEC2	**T1**	0.84	0.66	0.12	-0.20	-0.36	N/A
	T2	0.74	0.86	0.29	-0.18	-0.50	N/A
	T3	0.24	0.65	0.78	0.23	-0.35	N/A
	T4	-0.12	0.11	0.71	0.79	0	N/A
	T5	-0.38	-0.54	-0.10	0.56	0.78	N/A
	T6	N/A	N/A	N/A	N/A	N/A	N/A

		HB3-Uns2					
		T1	**T2**	**T3**	**T4**	**T5**	**T6**
HB3-HBEC-TNF	**T1**	0.88	0.63	0.12	-0.21	-0.32	0.38
	T2	0.26	0.72	0.83	0.28	-0.50	-0.45
	T3	0.73	0.89	0.34	-0.17	-0.51	0.05
	T4	-0.21	0.11	0.71	0.83	-0.09	-0.55
	T5	-0.46	-0.54	-0.07	0.59	0.76	0.1
	T6	-0.01	-0.46	-0.49	-0.11	0.7	0.72

		3D7-Uns					
		T1	**T2**	**T3**	**T4**	**T5**	**T6**
3D7-HBEC	**T1**	0.75	0.77	0.68	0.39	-0.2	-0.3
	T2	0.71	0.88	0.81	0.39	-0.35	-0.48
	T3	0.52	0.73	0.93	0.68	-0.13	-0.51
	T4	0.19	0.38	0.64	0.94	0.40	-0.37
	T5	-0.39	-0.31	-0.17	0.39	0.96	0.33
	T6	-0.24	-0.45	-0.49	-0.26	0.45	0.92

		IT-Uns					
		T1	**T2**	**T3**	**T4**	**T5**	**T6**
IT-HBEC	**T1**	0.91	0.63	0.17	-0.18	-0.37	0.17
	T2	0.84	0.93	0.43	-0.16	-0.58	-0.1
	T3	0.36	0.7	0.92	0.29	-0.46	-0.39
	T4	-0.19	0.03	0.73	0.89	0.18	-0.34
	T5	-0.5	-0.58	-0.12	0.68	0.89	0.11
	T6	-0.33	-0.58	-0.5	0.1	0.86	0.51

Figure S3

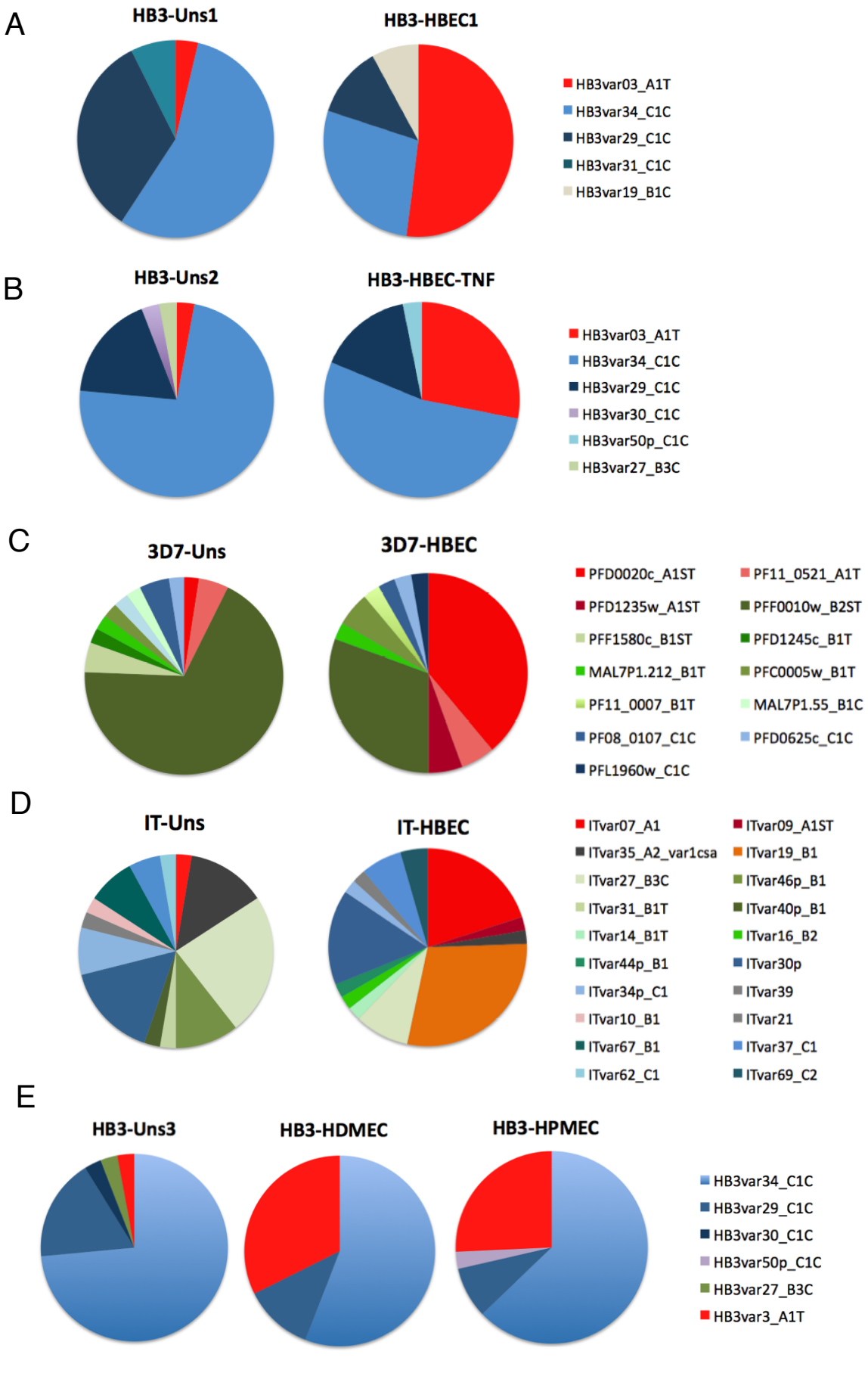
A
HB3-Uns1
HB3-HBEC1
HB3var03_A1T
HB3var34_C1C
HB3var29_C1C
HB3var31_C1C
HB3var19_B1C
B
HB3-Uns2
HB3-HBEC-TNF
HB3var03_A1T
HB3var34_C1C
HB3var29_C1C
HB3var30_C1C
HB3var50p_C1C
HB3var27_B3C
C
3D7-Uns
3D7-HBEC
PFD0020c_A1ST
PF11_0521_A1T
PFD1235w_A1ST
PFF0010w_B2ST
PFF1580c_B1ST
PFD1245c_B1T
MAL7P1.212_B1T
PFC0005w_B1T
PF11_0007_B1T
MAL7P1.55_B1C
PF08_0107_C1C
PFD0625c_C1C
PFL1960w_C1C
D
IT-Uns
IT-HBEC
ITvar07_A1
ITvar09_A1ST
ITvar35_A2_var1csa
ITvar19_B1
ITvar27_B3C
ITvar46p_B1
ITvar31_B1T
ITvar40p_B1
ITvar14_B1T
ITvar16_B2
ITvar44p_B1
ITvar30p
ITvar34p_C1
ITvar39
ITvar10_B1
ITvar21
ITvar67_B1
ITvar37_C1
ITvar62_C1
ITvar69_C2
E
HB3-Uns3
HB3-HDMEC
HB3-HPMEC
HB3var34_C1C
HB3var29_C1C
HB3var30_C1C
HB3var50p_C1C
HB3var27_B3C
HB3var3_A1T

Figure S4

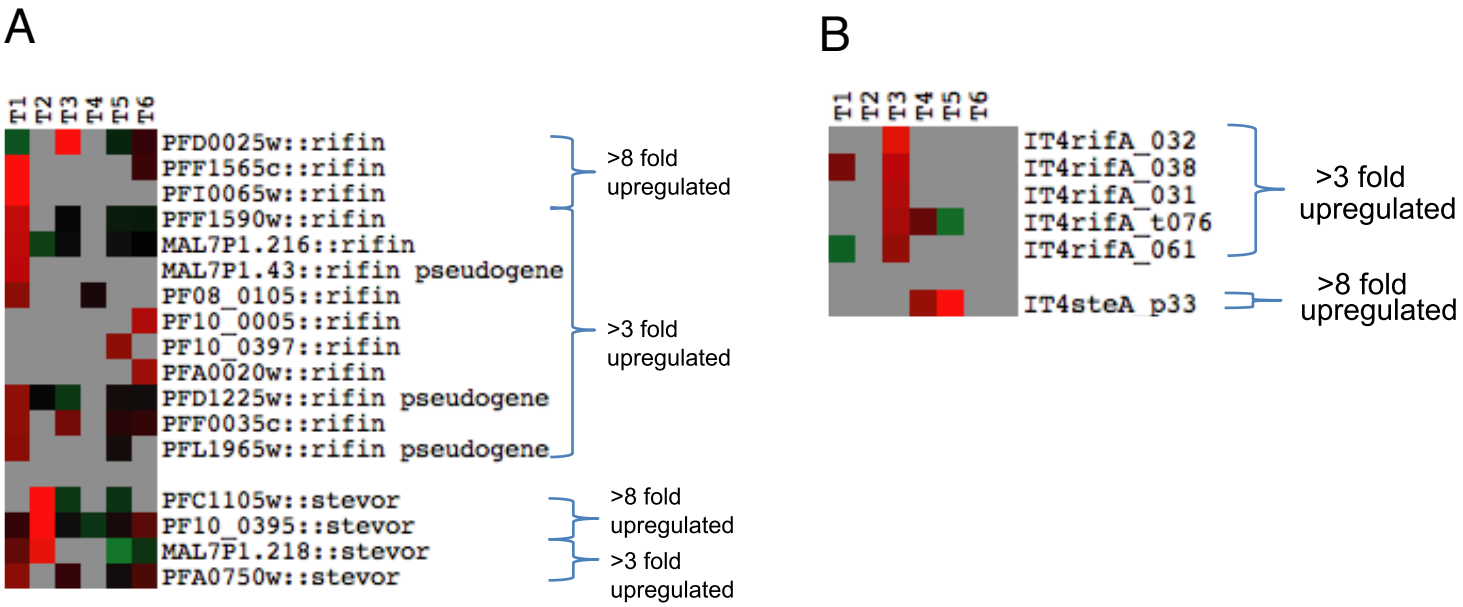
A
T1
T2
T3
T4
T5
T6
PFD0025w::rifin
PFF1565c::rifin
PFI0065w::rifin
PFF1590w::rifin
MAL7P1.216::rifin
MAL7P1.43::rifin pseudogene
PF08_0105::rifin
PF10_0005::rifin
PF10_0397::rifin
PFA0020w::rifin
PFD1225w::rifin pseudogene
PFF0035c::rifin
PFL1965w::rifin pseudogene
PFC1105w::stevor
PF10_0395::stevor
MAL7P1.218::stevor
PFA0750w::stevor
>8 fold upregulated
>3 fold upregulated
>8 fold upregulated
>3 fold upregulated
B
T1
T2
T3
T4
T5
T6
IT4rifA_032
IT4rifA_038
IT4rifA_031
IT4rifA_t076
IT4rifA_061
IT4steA p33
>3 fold upregulated
>8 fold upregulated

Figure S5.

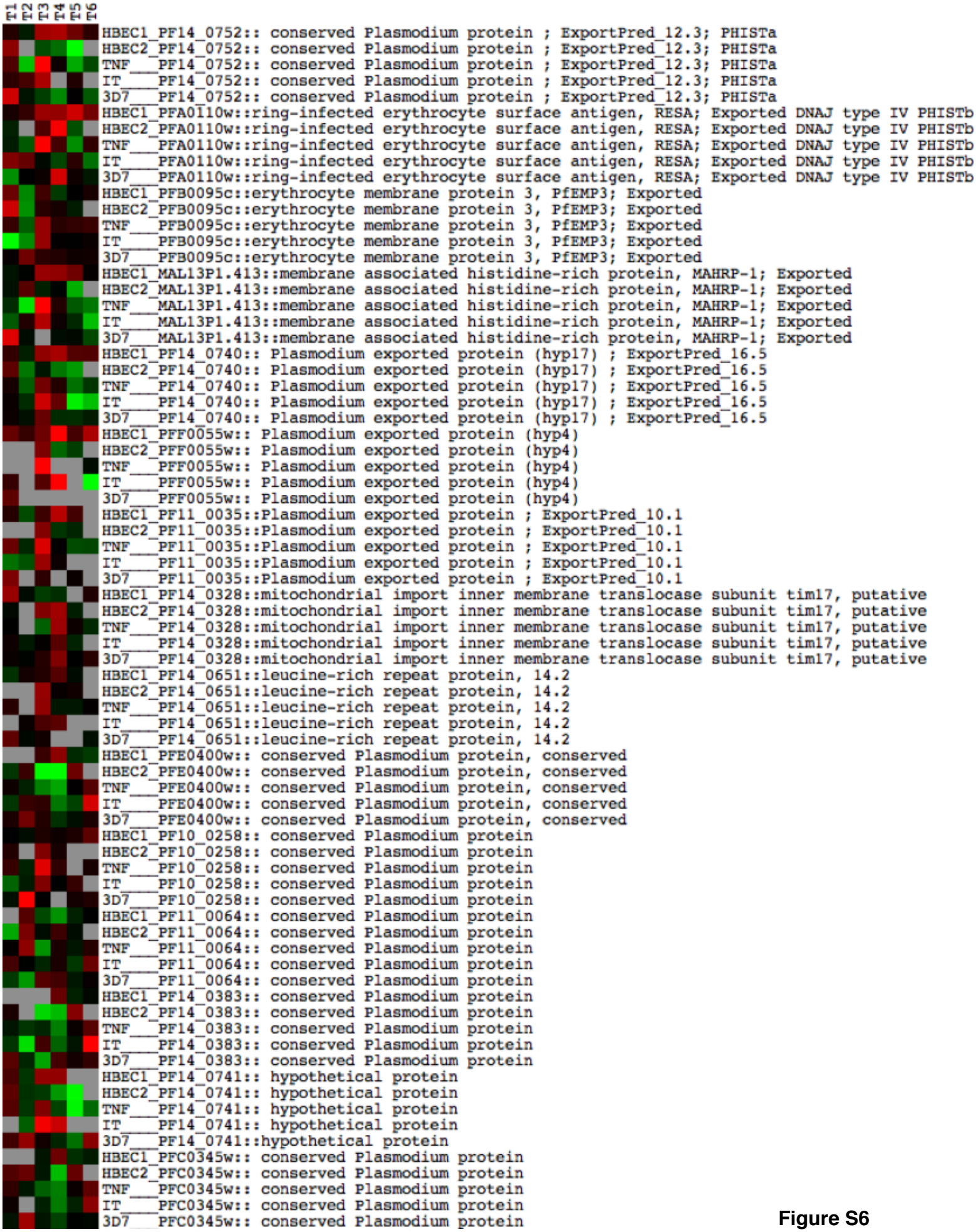
E1 E2 E3 E4 E5 E6
HBEC1_PF14_0752:: conserved Plasmodium protein ; ExportPred_12.3; PHISTa
HBEC2_PF14_0752:: conserved Plasmodium protein ; ExportPred_12.3; PHISTa
TNF___PF14_0752:: conserved Plasmodium protein ; ExportPred_12.3; PHISTa
IT___PF14_0752:: conserved Plasmodium protein ; ExportPred_12.3; PHISTa
3D7___PF14_0752:: conserved Plasmodium protein ; ExportPred_12.3; PHISTa
HBEC1_PFA0110w::ring-infected erythrocyte surface antigen, RESA; Exported DNAJ type IV PHISTb
HBEC2_PFA0110w::ring-infected erythrocyte surface antigen, RESA; Exported DNAJ type IV PHISTb
TNF___PFA0110w::ring-infected erythrocyte surface antigen, RESA; Exported DNAJ type IV PHISTb
IT___PFA0110w::ring-infected erythrocyte surface antigen, RESA; Exported DNAJ type IV PHISTb
3D7___PFA0110w::ring-infected erythrocyte surface antigen, RESA; Exported DNAJ type IV PHISTb
HBEC1_PFB0095c::erythrocyte membrane protein 3, PfEMP3; Exported
HBEC2_PFB0095c::erythrocyte membrane protein 3, PfEMP3; Exported
TNF___PFB0095c::erythrocyte membrane protein 3, PfEMP3; Exported
IT___PFB0095c::erythrocyte membrane protein 3, PfEMP3; Exported
3D7___PFB0095c::erythrocyte membrane protein 3, PfEMP3; Exported
HBEC1_MAL13P1.413::membrane associated histidine-rich protein, MAHRP-1; Exported
HBEC2_MAL13P1.413::membrane associated histidine-rich protein, MAHRP-1; Exported
TNF___MAL13P1.413::membrane associated histidine-rich protein, MAHRP-1; Exported
IT___MAL13P1.413::membrane associated histidine-rich protein, MAHRP-1; Exported
3D7___MAL13P1.413::membrane associated histidine-rich protein, MAHRP-1; Exported
HBEC1_PF14_0740:: Plasmodium exported protein (hyp17) ; ExportPred_16.5
HBEC2_PF14_0740:: Plasmodium exported protein (hyp17) ; ExportPred_16.5
TNF___PF14_0740:: Plasmodium exported protein (hyp17) ; ExportPred_16.5
IT___PF14_0740:: Plasmodium exported protein (hyp17) ; ExportPred_16.5
3D7___PF14_0740:: Plasmodium exported protein (hyp17) ; ExportPred_16.5
HBEC1_PFF0055w:: Plasmodium exported protein (hyp4)
HBEC2_PFF0055w:: Plasmodium exported protein (hyp4)
TNF___PFF0055w:: Plasmodium exported protein (hyp4)
IT___PFF0055w:: Plasmodium exported protein (hyp4)
3D7___PFF0055w:: Plasmodium exported protein (hyp4)
HBEC1_PF11_0035::Plasmodium exported protein ; ExportPred_10.1
HBEC2_PF11_0035::Plasmodium exported protein ; ExportPred_10.1
TNF___PF11_0035::Plasmodium exported protein ; ExportPred_10.1
IT___PF11_0035::Plasmodium exported protein ; ExportPred_10.1
3D7___PF11_0035::Plasmodium exported protein ; ExportPred_10.1
HBEC1_PF14_0328::mitochondrial import inner membrane translocase subunit tim17, putative
HBEC2_PF14_0328::mitochondrial import inner membrane translocase subunit tim17, putative
TNF___PF14_0328::mitochondrial import inner membrane translocase subunit tim17, putative
IT___PF14_0328::mitochondrial import inner membrane translocase subunit tim17, putative
3D7___PF14_0328::mitochondrial import inner membrane translocase subunit tim17, putative
HBEC1_PF14_0651::leucine-rich repeat protein, 14.2
HBEC2_PF14_0651::leucine-rich repeat protein, 14.2
TNF___PF14_0651::leucine-rich repeat protein, 14.2
IT___PF14_0651::leucine-rich repeat protein, 14.2
3D7___PF14_0651::leucine-rich repeat protein, 14.2
HBEC1_PFE0400w:: conserved Plasmodium protein, conserved
HBEC2_PFE0400w:: conserved Plasmodium protein, conserved
TNF___PFE0400w:: conserved Plasmodium protein, conserved
IT___PFE0400w:: conserved Plasmodium protein, conserved
3D7___PFE0400w:: conserved Plasmodium protein, conserved
HBEC1_PF10_0258:: conserved Plasmodium protein
HBEC2_PF10_0258:: conserved Plasmodium protein
TNF___PF10_0258:: conserved Plasmodium protein
IT___PF10_0258:: conserved Plasmodium protein
3D7___PF10_0258:: conserved Plasmodium protein
HBEC1_PF11_0064:: conserved Plasmodium protein
HBEC2_PF11_0064:: conserved Plasmodium protein
TNF___PF11_0064:: conserved Plasmodium protein
IT___PF11_0064:: conserved Plasmodium protein
3D7___PF11_0064:: conserved Plasmodium protein
HBEC1_PF14_0383:: conserved Plasmodium protein
HBEC2_PF14_0383:: conserved Plasmodium protein
TNF___PF14_0383:: conserved Plasmodium protein
IT___PF14_0383:: conserved Plasmodium protein
3D7___PF14_0383:: conserved Plasmodium protein
HBEC1_PF14_0741:: hypothetical protein
HBEC2_PF14_0741:: hypothetical protein
TNF___PF14_0741:: hypothetical protein
IT___PF14_0741:: hypothetical protein
3D7___PF14_0741::hypothetical protein
HBEC1_PFC0345w:: conserved Plasmodium protein
HBEC2_PFC0345w:: conserved Plasmodium protein
TNF___PFC0345w:: conserved Plasmodium protein
IT___PFC0345w:: conserved Plasmodium protein
3D7___PFC0345w:: conserved Plasmodium protein

Figure S6

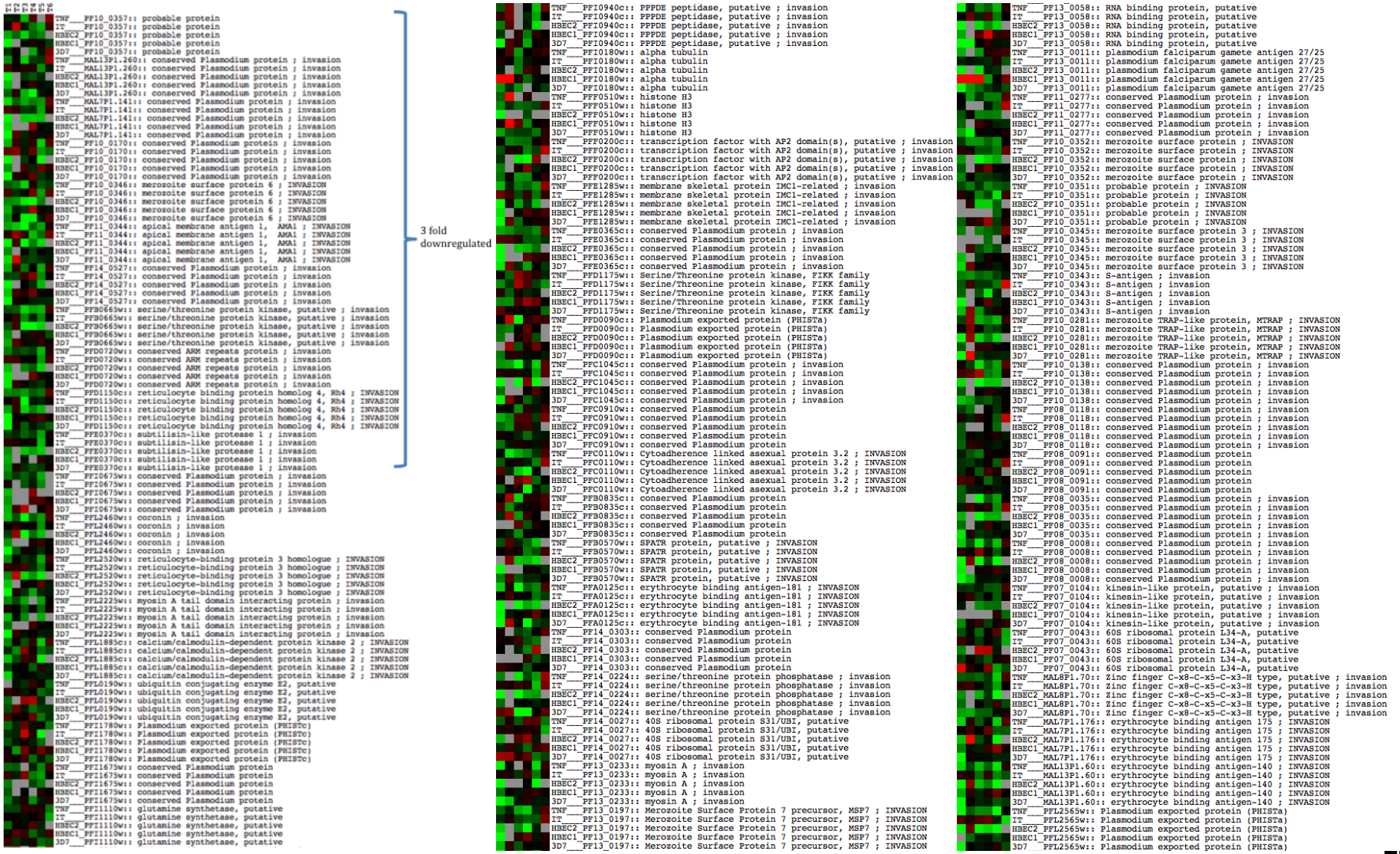

Figure S7

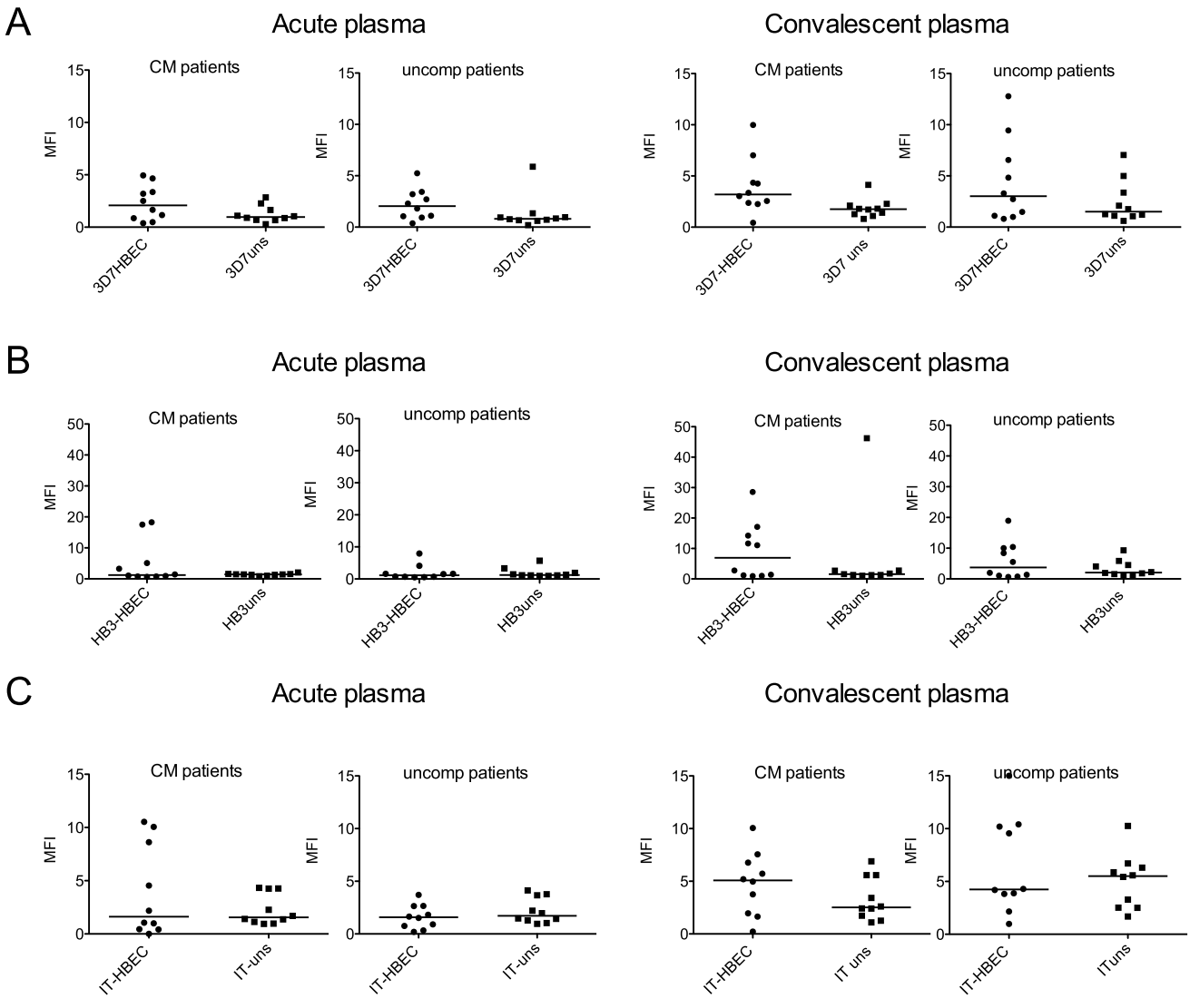

D

	Median MFI HBEC	IQR	Median MFI Uns	IQR	P value
3D7 parasites					
Acute plasma CM	2.08	0.77-3.68	0.97	0.69-1.81	0.17
Acute plasma UM	2.05	1.03-3.27	0.81	0.65-1.06	**0.04**
Conv plasma CM	3.20	2.30-5.01	1.76	1.22-2.15	**0.009**
Conv plasma UM	3.02	1.07-7.28	1.50	1.09-3.77	0.44
HB3 parasites					
Acute plasma CM	1.24	0.79-8.22	1.44	1.23-1.57	0.85
Acute plasma UM	1.14	0.64-2.23	1.24	1.06-2.25	0.48
Conv plasma CM	6.92	1.14-14.93	1.57	1.28-2.76	0.60
Conv plasma UM	3.74	0.99-10.12	2.07	4.85	0.74
IT parasites					
Acute plasma CM	1.62	0.44-8.98	1.55	1.09-4.26	1.00
Acute plasma UM	1.58	0.65-2.65	1.72	1.22-3.69	0.35
Conv plasma CM	5.08	1.87-6.96	2.51	1.61-5.58	0.32
Conv plasma UM	4.25	3.41-10.25	5.51	2.52-6.41	0.74

Figure S8